A New Normal for Interest Rates? Evidence from Inflation-Indexed Debt

Jens H. E. Christensen

and

Glenn D. Rudebusch

Abstract

Some have argued that Treasury yields have been pushed down by lower longer-run expectations of the safe, short-term real interest rate—that is, by a drop in the so-called equilibrium or natural rate of interest. We examine this possibility using an arbitrage-free dynamic term structure model estimated directly on prices of individual inflation-indexed bonds with adjustments for real term and liquidity risk premiums. We find that a lower expected short real rate has accounted for about 2 percentage points of the general downtrend in yields over the past two decades and that this situation seems unlikely to reverse quickly.

JEL Classification: C32, E43, E52, G12

Keywords: affine term structure model, U.S. Treasury inflation-protected securities (TIPS), financial market frictions, monetary policy

Jens H. E. Christensen (jens.christensen.sf.frb.org), Glenn D. Rudebusch (glenn.rudebusch@sf.frb.org): Economic Research Department, Federal Reserve Bank of San Francisco, 101 Market Street (MS 1130), San Francisco, CA 94105. We thank Vasco Cúrdia for helpful comments on an earlier draft of the paper. Furthermore, we thank Helen Irvin, Patrick Shultz, and Logan Tribull for excellent research assistance. The views in this paper are solely the responsibility of the authors and do not necessarily reflect those of others in the Federal Reserve System.

This version: March 22, 2017.

1 Introduction

The general level of U.S. interest rates has gradually declined over the past few decades. In the 1980s and 1990s, falling inflation expectations played a key role in this decline. But more recently, actual inflation as well as survey-based measures of longer-run inflation expectations have both stabilized at around 2 percent. Therefore, researchers have argued that the decline in interest rates since 2000 reflects a variety of longer-run real-side factors instead of nominal ones. These real factors—such as slower productivity growth and an aging population—affect global saving and investment and can push down nominal and real yield curves by lowering the steady-state level of the safe short-term real interest rate.[1] This steady-state real rate is often called the equilibrium or natural or neutral rate of interest and is commonly defined as the short-term real rate of return that would prevail in the absence of transitory disturbances. However, some have dismissed the evidence for a new lower equilibrium real rate. They downplay the role of persistent real-side factors and argue that yields have been held down recently by temporary factors such as the headwinds from credit deleveraging in the aftermath of the financial crisis.[2] So far, this ongoing debate has focused on estimates drawn from *macroeconomic* models and data. In this paper, we use *financial* models and data to provide an alternative perspective on a possible lower new normal for interest rates.

The issue of whether there has been a persistent shift in the equilibrium real rate is of widespread significance. For investors, the steady-state level of the real short rate serves as an important anchor for projections of the future discount rates used in valuing assets (e.g., Clarida 2014). For policymakers and researchers, the equilibrium or natural rate of interest is a policy lodestar that provides a neutral benchmark to calibrate the stance of monetary policy: Monetary policy is expansionary if the short-term real interest rate lies below the natural rate and contractionary if it lies above. A good estimate of the equilibrium real rate is also necessary to operationalize popular monetary policy rules such as the Taylor rule.[3] More broadly, during the past decade or so, the possibility of a lower new normal for interest rates has been at the center of key policy debates about the bond market conundrum, the global saving glut, and secular stagnation.[4]

Given the importance of the steady-state real interest rate, many researchers have used macroeconomic models and data to try to pin it down. The best known of these—Laubach

[1]For example, see Rachel and Smith (2015), Gagnon et al. (2016), Hamilton et al. (2016), Laubach and Williams (2016), and Pescatori and Turunen (2016) among many others.

[2]For example, see Kiley (2015), Lo and Rogoff (2015), and Taylor and Wieland (2016).

[3]For recent discussions by Federal Reserve policymakers describing the connection between the natural rate of interest and monetary policy, see, e.g., Yellen (2015), Fischer (2016), and Williams (2016). For research on the role of the natural rate in monetary policy, see Rudebusch (2001), Orphanides and Williams (2002), Eggertsson et al. (2016), and Hamilton et al. (2016), among many others.

[4]See, for example, Greenspan (2005), Bernanke (2005), and Summers (2014, 2015), respectively, on these three debates.

and Williams (2003, 2016)—infers the equilibrium real short rate using the Rudebusch and Svensson (1999) macroeconomic model and aggregate data on a nominal short-term interest rate, consumer price inflation, and the output gap. As Laubach and Williams (2016, p. 57) define it, the natural rate of interest is based on "a 'longer-run' perspective, in that it refers to the level of the real interest rate expected to prevail, say, five to 10 years in the future, after the economy has emerged from any cyclical fluctuations and is expanding at its trend rate." They use the Kalman filter to distinguish trend and cycle in the real rate using the definition of the neutral stance of monetary policy above. Similarly, Johannsen and Mertens (2016) and Lubick and Matthes (2015) provide closely related natural rate estimates from a filtering of the macroeconomic data in the context of macroeconomic models. Other macroeconomic researchers, such as Cúrdia et al. (2015), take a more structural approach and use a dynamic stochastic general equilibrium (DSGE) model to estimate the equilibrium real rate.

However, the various macro-based approaches for identifying a new lower equilibrium real rate all have several well-known shortcomings. First, as emphasized by Kiley (2015) and Taylor and Wieland (2016), the macro-based estimates of the natural rate will be distorted by any model misspecifications, especially in the assumed output and inflation dynamics. Such model misspecifications could also arise from ignoring any structural breaks during the sample including, for example, the episodic constraints associated with the zero lower bound on nominal rates. Second, Kiley (2015) finds that the key relationship underlying the macro-based estimates—that is, the connection between real rate and output gaps—appears to be a weak empirical foundation for learning much about the natural rate of interest. Third, Laubach and Williams (2003) and Kiley (2015) stress the particular econometric difficulties of estimating a permanent component in these circumstances—the so-called pile-up problem. Finally, as noted by Clark and Kozicki (2005), a macro-based approach has a number of problems from the standpoint of a real-time analysis. For example, the macro-based estimates use extensively-revised output and inflation data to create equilibrium real rate estimates that would not have been available historically. In addition, the macro-based estimates do not include any forward-looking financial data, and a backward-looking, one-sided filtering applied in real time will face difficulties in distinguishing persistent shifts in the economy that affect the natural rate from cyclical and transitory fluctuations.

Given this litany of criticisms of macro-based estimation, we turn to financial models and data to provide a new, forward-looking approach to estimate the equilibrium real rate of interest. To incorporate financial market information, we use the prices of inflation-indexed debt, namely, U.S. Treasury Inflation-Protected Securities (TIPS), which have coupon and principal payments that are indexed to the Consumer Price Index (CPI) and are available after 1997 when the TIPS program was launched. These securities compensate investors for the erosion of purchasing power due to price inflation, so their bond prices can be expressed

directly in terms of real yields. We assume that the longer-term expectations embedded in TIPS prices reflect financial market participants' views about the steady state of the economy including the natural rate of interest. Our financial market measure of the natural rate has the advantage that it can be obtained in real time at the same high frequency as the underlying bond price data. Furthermore, our analysis uses prices of individual bonds rather than the more usual input of yields from fitted synthetic curves. This technique is particularly useful for analyzing inflation-indexed debt at times when only a limited sample of bonds may be available.

Still, the use of TIPS for measuring the steady-state short-term real interest rate poses its own empirical challenges. One problem is that inflation-indexed bond prices include a real term premium. Given the generally upward slope of the TIPS yield curve, the real term premium is usually positive. However, little is known with certainty about its size or variability. In addition, despite the fairly large notional amount of outstanding TIPS, these securities face appreciable liquidity risk. For example, Fleming and Krishnan (2012) report that TIPS usually have a smaller trading volume and wider bid-ask spreads than nominal Treasury bonds. Presumably, investors require a premium for bearing the liquidity risk associated with holding TIPS, but the extent and time variation of this liquidity premium remain under investigation.[5]

To estimate the natural rate of interest in the presence of liquidity and real term premiums, we use an arbitrage-free dynamic term structure model of real yields augmented with a liquidity risk factor. The identification of the liquidity risk factor comes from its unique loading for each individual TIPS security as in Andreasen, Christensen, and Riddell (2017, henceforth ACR). The underlying mechanism assumes that, over time, an increasing proportion of the outstanding inventory is locked up in buy-and-hold portfolios. Given forward-looking investor behavior, this lock-up effect means that a particular bond's sensitivity to the market-wide liquidity factor will vary depending on how seasoned the bond is and how close to maturity it is. By observing a cross section of TIPS prices over time—each with a different time-since-issuance and time-to-maturity—the liquidity factor can be identified. The theoretical arbitrage-free formulation of the model also provides identification of a time-varying real term premium in the pricing of TIPS. Identifying the liquidity premium and real term premium allows us to estimate the underlying frictionless real rate term structure and the natural rate of interest, which we measure as the average expected real short rate over a five-year period starting five years ahead. Our preferred estimate of the natural rate of interest, r_t^*, is shown in Figure 1 along with 10-year nominal and real Treasury yields. Both nominal and real long-term yields have trended down together over the past two decades, and this

[5]See, for example, Sack and Elsasser (2004), Campbell et al. (2009), Dudley et al. (2009), Gürkaynak et al. (2010), Pflueger and Viceira (2013), and Fleckenstein et al. (2014).

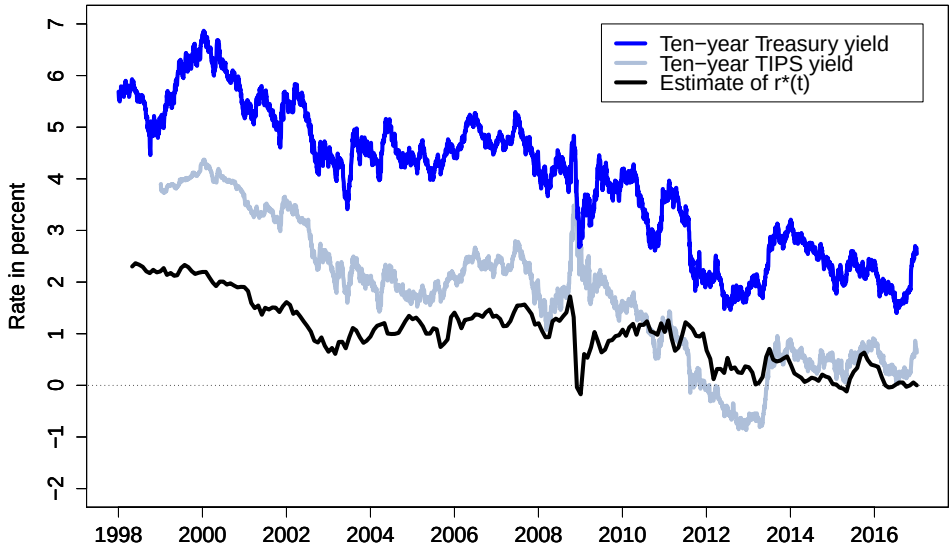

Figure 1: **Long-Term Treasury and TIPS Yields and an Estimate of r***
Ten-year nominal and real (TIPS) Treasury yields from Gürkaynak et al. (2007, 2010) databases and our preferred our T-O-L model estimate of the equilibrium real short rate, r_t^*, i.e., the 5-to-10 year risk-neutral real rate.

concurrence suggests little net change in inflation expectations or the inflation risk premium. The estimated equilibrium real rate falls from just over 2 percent to zero during this period. Accordingly, our results show that about half of the 4-percentage-point decline in longer-term Treasury yields represents a reduction in the natural rate of interest. Our model estimates also suggest that this situation is unlikely to reverse quickly in the years ahead.

Our analysis focuses on a real term structure model that only includes the prices of inflation-indexed TIPS. This contrasts with previous TIPS research that has jointly modeled both the real and nominal yield curves, including Christensen et al. (2010), D'Amico et al. (2014), and Abrahams et al. (2016). Such joint specifications can also be used to estimate the steady-state real rate—though this earlier work has emphasized only the measurement of inflation expectations and risk. Relative to our procedure of using just TIPS to estimate the natural rate, including both real and nominal yields has the advantage of being able to estimate a model on a much larger sample of bond yields. However, a joint specification also requires additional modeling structure—including specifying more pricing factors, an inflation risk premium, and inflation expectations. The greater number of modeling elements—along with the requirement that this more elaborate structure remains stable over the sample—raise the risk of model misspecification, which can contaminate estimates of the natural rate and

model inference more generally. In particular, if the inflation components are misspecified, the whole dynamic system may be compromised. Furthermore, during the period from 2009 to 2015 when the Federal Reserve kept the overnight federal funds rate at its effective zero lower bound, the dynamic interactions of short- and medium-term *nominal* Treasury yields were affected. Such a constraint is very difficult to include in an empirical term structure model of nominal yields (see Swanson and Williams 2014 and Christensen and Rudebusch 2015 for discussions). By relying solely on real TIPS yields, which are not subject to a lower bound, we avoid this complication altogether. Still, for completeness, we compare the natural rate estimates below from a TIPS-only specification and from joint representations of the real and nominal yield curves.

The analysis in this paper relates to several important literatures. Most directly, it speaks to the burgeoning literature on measurement of the natural rate of interest. Second, our estimates of the real yield curve that would prevail without trading frictions have implications for asset pricing analysis on the true slope of the real yield curve. Finally, our results relate to research on financial market liquidity. Indeed, the TIPS liquidity premiums we estimate may serve as a useful benchmark for assessing liquidity premiums in other fixed-income markets.

The remainder of the paper is organized as follows. Section 2 describes our definition of the natural rate and our theoretical framework, which adjusts TIPS yields for real term premiums and liquidity premiums. This section provides a description of the no-arbitrage term structure model we use and its extension with a liquidity risk factor. Section 3 contains a description of the TIPS data, while Section 4 presents the empirical results. Section 5 analyzes our TIPS-based estimate of the natural rate and compares it with other measures. Finally, Section 6 concludes. Appendices contain additional technical details on TIPS pricing, TIPS characteristics, and model estimation.

2 Identifying the Natural Rate of Interest with TIPS

In this section, we first describe how real bond yields can be decomposed into the underlying real rate expectations component and a residual real term premium in a world without any trading frictions. This model of frictionless dynamics is fundamental to our analysis. We then describe the wedge between the theoretical frictionless real yields and the observed TIPS yields caused by imperfect bond market liquidity. Finally, we augment the frictionless model to adjust TIPS yields for the liquidity bias.

2.1 Decomposing Real Yields with Frictionless Affine Models

We begin our analysis assuming a world with no frictions to the trading of financial claims; therefore, there are no bid-ask spreads, and any financial claim can be traded in arbitrarily

small or large amounts without affecting its price. As a consequence, with no liquidity risk to be rewarded, financial market prices contain no liquidity premiums. Under such ideal conditions, real yields vary either because fundamental factors in the economy have changed or because investors have altered their perceptions of, or aversions to, the risks that those economic fundamentals represent.

Assessing the variation in real yields caused by time-varying real term premiums requires an accurate model of expectations for the instantaneous risk-free real rate r_t and the term premium. For simplicity, we focus on decomposing $P_t(\tau)$, the price of a zero-coupon real bond at time t that has a single payoff, namely one consumption unit, at maturity $t+\tau$. Under standard assumptions, this price is given by

$$P_t(\tau) = E_t^P\Big[\frac{M_{t+\tau}}{M_t}\Big],$$

where the stochastic discount factor, M_t, denotes the value at time t_0 of a real claim (one measured in consumption units) at a future date t, and the superscript P refers to the actual, or real-world, probability measure underlying the dynamics of M_t.

Our definition of the natural rate of interest r_t^* is

$$r_t^* = \frac{1}{5}\int_{t+5}^{t+10} E_t^P[r_{t+s}]ds, \tag{1}$$

that is, the average expected real short rate over a five-year period starting five years ahead where the expectation is with respect to the objective P-probability measure. This 5yr5yr forward average expected real short rate should be little affected by short-term transitory shocks. In the empirical analysis, we rely on the market prices of TIPS to construct this market-based measure of the natural rate. In doing so, it is important to acknowledge that financial market prices do not reflect objective P-expectations as in equation (1). Instead, they reflect expectations adjusted with the premiums investors demand for being exposed to the underlying risks.

We follow the usual empirical finance approach that models bond prices with latent factors, here denoted as X_t, and the assumption of no residual arbitrage opportunities.[6] We assume that X_t follows an affine Gaussian process with constant volatility, with dynamics in continuous time given by the solution to the following stochastic differential equation (SDE):

$$dX_t = K^P(\theta^P - X_t) + \Sigma dW_t^P,$$

where K^P is an $n \times n$ mean-reversion matrix, θ^P is an $n \times 1$ vector of mean levels, Σ is an

[6] Ultimately, of course, the behavior of the stochastic discount factor is determined by the preferences of the agents in the economy, as in, for example, Rudebusch and Swanson (2011).

$n \times n$ volatility matrix, and W_t^P is an n-dimensional Brownian motion. The dynamics of the stochastic discount function are given by

$$dM_t = r_t M_t dt + \Gamma_t' M_t dW_t^P,$$

and the instantaneous risk-free real rate, r_t, is assumed affine in the state variables

$$r_t = \delta_0 + \delta_1 X_t,$$

where $\delta_0 \in \mathbf{R}$ and $\delta_1 \in \mathbf{R}^n$. The risk premiums, Γ_t, are also affine

$$\Gamma_t = \gamma_0 + \gamma_1 X_t,$$

where $\gamma_0 \in \mathbf{R}^n$ and $\gamma_1 \in \mathbf{R}^{n \times n}$.

Duffie and Kan (1996) show that these assumptions imply that zero-coupon real yields are also affine in X_t:

$$y_t(\tau) = -\frac{1}{\tau} A(\tau) - \frac{1}{\tau} B(\tau)' X_t,$$

where $A(\tau)$ and $B(\tau)$ are given as solutions to the following system of ordinary differential equations

$$\begin{aligned} \frac{dB(\tau)}{d\tau} &= -\delta_1 - (K^P + \Sigma\gamma_1)' B(\tau), \quad B(0) = 0, \\ \frac{dA(\tau)}{d\tau} &= -\delta_0 + B(\tau)'(K^P\theta^P - \Sigma\gamma_0) + \frac{1}{2}\sum_{j=1}^{n} \left(\Sigma' B(\tau) B(\tau)' \Sigma\right)_{j,j}, \quad A(0) = 0. \end{aligned}$$

Thus, the $A(\tau)$ and $B(\tau)$ functions are calculated *as if* the dynamics of the state variables had a constant drift term equal to $K^P\theta^P - \Sigma\gamma_0$ instead of the actual $K^P\theta^P$ and a mean-reversion matrix equal to $K^P + \Sigma\gamma_1$ as opposed to the actual K^P.[7] The difference is determined by the risk premium Γ_t and reflects investors' aversion to the risks embodied in X_t.

Finally, we define the real term premium as

$$TP_t(\tau) = y_t(\tau) - \frac{1}{\tau}\int_t^{t+\tau} E_t^P[r_s] ds. \tag{2}$$

That is, the real term premium is the difference in expected real return between a buy and hold strategy for a τ-year real bond and an instantaneous rollover strategy at the risk-free real rate r_t. This model thus decomposes yields into a real term premium and real short rate expectations component, which can then be used to obtain the natural rate via equation (1).

[7] The probability measure with these alternative dynamics is frequently referred to as the risk-neutral, or Q, probability measure since the expected return on any asset under this measure is equal to the risk-free real rate r_t that a risk-neutral investor would demand.

2.2 A Frictionless Arbitrage-Free Model of Real Yields

To capture the fundamental factors operating the frictionless real yield curve described above, we choose to focus on the tractable affine dynamic term structure model introduced in Christensen et al. (2011). Although the model is not formulated using the canonical form of affine term structure models introduced by Dai and Singleton (2000), it can be viewed as a restricted version of the canonical Gaussian model.[8]

In this arbitrage-free Nelson-Siegel (AFNS) model, the state vector is denoted by $X_t = (L_t, S_t, C_t)$, where L_t is a level factor, S_t is a slope factor, and C_t is a curvature factor. The instantaneous risk-free real rate is defined as

$$r_t = L_t + S_t. \tag{3}$$

The risk-neutral (or Q-) dynamics of the state variables are given by the stochastic differential equations[9]

$$\begin{pmatrix} dL_t \\ dS_t \\ dC_t \end{pmatrix} = \begin{pmatrix} 0 & 0 & 0 \\ 0 & -\lambda & \lambda \\ 0 & 0 & -\lambda \end{pmatrix} \begin{pmatrix} L_t \\ S_t \\ C_t \end{pmatrix} dt + \Sigma \begin{pmatrix} dW_t^{L,Q} \\ dW_t^{S,Q} \\ dW_t^{C,Q} \end{pmatrix}, \tag{4}$$

where Σ is the constant covariance (or volatility) matrix.[10] Based on this specification of the Q-dynamics, zero-coupon real bond yields preserve the Nelson-Siegel factor loading structure as

$$y_t(\tau) = L_t + \left(\frac{1-e^{-\lambda\tau}}{\lambda\tau}\right) S_t + \left(\frac{1-e^{-\lambda\tau}}{\lambda\tau} - e^{-\lambda\tau}\right) C_t - \frac{A(\tau)}{\tau}, \tag{5}$$

where the yield-adjustment term is given by

$$\begin{aligned} \frac{A(\tau)}{\tau} &= \frac{\sigma_{11}^2}{6}\tau^2 + \sigma_{22}^2\Big[\frac{1}{2\lambda^2} - \frac{1}{\lambda^3}\frac{1-e^{-\lambda\tau}}{\tau} + \frac{1}{4\lambda^3}\frac{1-e^{-2\lambda\tau}}{\tau}\Big] \\ &\quad + \sigma_{33}^2\Big[\frac{1}{2\lambda^2} + \frac{1}{\lambda^2}e^{-\lambda\tau} - \frac{1}{4\lambda}\tau e^{-2\lambda\tau} - \frac{3}{4\lambda^2}e^{-2\lambda\tau} + \frac{5}{8\lambda^3}\frac{1-e^{-2\lambda\tau}}{\tau} - \frac{2}{\lambda^3}\frac{1-e^{-\lambda\tau}}{\tau}\Big]. \end{aligned}$$

To complete the description of the model and to implement it empirically, we will need to specify the risk premiums that connect these factor dynamics under the Q-measure to the dynamics under the real-world (or physical) P-measure. It is important to note that there are no restrictions on the dynamic drift components under the empirical P-measure beyond the requirement of constant volatility. To facilitate empirical implementation, we use the essentially affine risk premium specification introduced in Duffee (2002). In the Gaussian

[8] See Christensen et al. (2011) for details on the derivation of the restrictions.

[9] As discussed in Christensen et al. (2011), with a unit root in the level factor, the model is not arbitrage-free with an unbounded horizon; therefore, as is often done theoretical discussions, we impose an arbitrary maximum horizon.

[10] As per Christensen et al. (2011), Σ is a diagonal matrix, and θ^Q is set to zero without loss of generality.

framework, this specification implies that the risk premiums Γ_t depend on the state variables; that is,

$$\Gamma_t = \gamma^0 + \gamma^1 X_t,$$

where $\gamma^0 \in \mathbf{R}^3$ and $\gamma^1 \in \mathbf{R}^{3\times 3}$ contain unrestricted parameters.

Thus, the resulting unrestricted three-factor AFNS model has P-dynamics given by

$$\begin{pmatrix} dL_t \\ dS_t \\ dC_t \end{pmatrix} = \begin{pmatrix} \kappa_{11}^P & \kappa_{12}^P & \kappa_{13}^P \\ \kappa_{21}^P & \kappa_{22}^P & \kappa_{23}^P \\ \kappa_{31}^P & \kappa_{32}^P & \kappa_{33}^P \end{pmatrix} \left(\begin{pmatrix} \theta_1^P \\ \theta_2^P \\ \theta_3^P \end{pmatrix} - \begin{pmatrix} L_t \\ S_t \\ C_t \end{pmatrix} \right) dt + \Sigma \begin{pmatrix} dW_t^{L,P} \\ dW_t^{S,P} \\ dW_t^{C,P} \end{pmatrix}.$$

This is the transition equation in the Kalman filter estimation.

2.3 An Arbitrage-Free Model of Real Yields with Liquidity Risk

Equation (2) highlights that the decomposition of real yields into expectations and risk premium components can be distorted if the observed real yields are biased by liquidity effects. In this section, we augment the TIPS-only (T-O) frictionless model introduced above to account for the liquidity risk of the TIPS prices we use in the empirical analysis. By adjusting the TIPS prices for liquidity effects we obtain estimates of the ideal or frictionless real yields that feature in the real yield decomposition in equation (2), which ultimately provides us with readings of the natural rate as defined in equation (1).

Due to the liquidity risk of TIPS, their yields are sensitive to liquidity pressures. As a consequence, the discounting of their future cash flows is not performed with the frictionless real discount function described in Section 2.1, but rather with a discount function that also accounts for liquidity risk. Recent research by Hu et al. (2013) and others suggest that liquidity is indeed a priced risk factor. Thus, we follow ACR and represent this by a single liquidity risk factor denoted X_t^{liq}.[11] Furthermore, the ACR approach assumes liquidity risk is security-specific in nature. Indeed, there is a unique function used to discount the cash flow of each TIPS indexed i, and it takes the following simple form:

$$\overline{r}_t^i = r_t + \beta^i (1 - e^{-\lambda^{L,i}(t-t_0^i)}) X_t^{liq}, \tag{6}$$

where r_t is the frictionless instantaneous real rate, t_0^i denotes the date of issuance of the security, β^i is its sensitivity to the variation in the liquidity risk factor, and $\lambda^{L,i}$ is a decay parameter. While we could expect the sensitivities to be identical across securities, the results reported by ACR show that it is important to allow for the possibility that the sensitivities differ across securities. Furthermore, we allow the decay parameter $\lambda^{L,i}$ to vary across secu-

[11] D'Amico et al. (2014) and Abrahams et al. (2016) also only allow for a single TIPS liquidity factor.

rities as well. Since β^i and $\lambda^{L,i}$ have a nonlinear relationship in the bond pricing formula to be detailed below, both are identified econometrically. Finally, we note that equation (6) can be combined with any dynamic term structure model to account for security-specific liquidity risks.

The inclusion of the issuance date t_0^i in the pricing formula captures the effect that, as time passes, an increasing fraction of a given security is held by buy-and-hold investors.[12] This limits the amount of the security available for trading and affects its sensitivity to the liquidity factor. Rational, forward-looking investors will take this dynamic pattern into consideration when they determine what they are willing to pay for the security at any given point in time between the date of issuance and the maturity of the bond. This dynamic pattern is built into the model structure.

To augment the T-O model to account for the liquidity risk in the pricing of TIPS as described, let $X_t = (L_t, S_t, C_t, X_t^{liq})$ denote the state vector of the four-factor TIPS-only with liquidity adjustment (T-O-L) model. As in the non-augmented model, we let the frictionless instantaneous real risk-free rate be defined by equation (3), while the risk-neutral dynamics of the state variables used for pricing are given by

$$\begin{pmatrix} dL_t \\ dS_t \\ dC_t \\ dX_t^{liq} \end{pmatrix} = \begin{pmatrix} 0 & 0 & 0 & 0 \\ 0 & \lambda & -\lambda & 0 \\ 0 & 0 & \lambda & 0 \\ 0 & 0 & 0 & \kappa_{liq}^Q \end{pmatrix} \left[\begin{pmatrix} 0 \\ 0 \\ 0 \\ \theta_{liq}^Q \end{pmatrix} - \begin{pmatrix} L_t \\ S_t \\ C_t \\ X_t^{liq} \end{pmatrix} \right] dt + \Sigma \begin{pmatrix} dW_t^{L,Q} \\ dW_t^{S,Q} \\ dW_t^{C,Q} \\ dW_t^{liq,Q} \end{pmatrix},$$

where Σ continues to be a diagonal matrix.

It follows from these Q-dynamics that TIPS yields are sensitive to liquidity risk. In particular, pricing of TIPS is not performed with the frictionless real discount function, but rather with the discount function that accounts for the liquidity risk as detailed earlier:

$$\overline{r}_t^i = r_t + \beta^i(1 - e^{-\lambda^{L,i}(t-t_0^i)})X_t^{liq} = L_t + S_t + \beta^i(1 - e^{-\lambda^{L,i}(t-t_0^i)})X_t^{liq}. \tag{7}$$

In Appendix A, we show that the net present value of one unit of consumption paid by TIPS i at time $t+\tau$ has the following exponential-affine form

$$\begin{aligned} P_t(t_0^i, \tau) &= E^Q\left[e^{-\int_t^{t+\tau} \overline{r}^i(s,t_0^i)ds}\right] \\ &= \exp\Big(B_1(\tau)L_t + B_2(\tau)S_t + B_3(\tau)C_t + B_4(t, t_0^i, \tau)X_t^{Liq} + A(t, t_0^i, \tau)\Big). \end{aligned}$$

This result implies that the model belongs to the class of Gaussian affine term structure

[12] Typically, at issuance, primary dealers make the bulk of the purchases of a security and little is locked up immediately. However, very close to when a bond matures, essentially all remaining investors have bought it to hold to maturity.

models, but unlike standard Gaussian models, $P_t(t_0^i, \tau^i)$ is time-inhomogeneous. Note also that, by fixing $\beta^i = 0$ for all i, we recover the T-O model.

Now, consider the whole value of TIPS i issued at time t_0^i with maturity at $t + \tau^i$ that pays an annual coupon C^i semi-annually. Its price is given by

$$\begin{aligned}\overline{P}_t(t_0^i, \tau^i, C^i) &= \frac{C^i}{2}\frac{(t_1 - t)}{1/2}E^Q\left[e^{-\int_t^{t_1}\overline{r}^{R,i}(s,t_0^i)ds}\right] + \sum_{j=2}^{N}\frac{C^i}{2}E^Q\left[e^{-\int_t^{t_j}\overline{r}^{R,i}(s,t_0^i)ds}\right] \\ &\quad + E^Q\left[e^{-\int_t^{t+\tau^i}\overline{r}^{R,i}(s,t_0^i)ds}\right].\end{aligned}$$

There are two minor omissions in this bond pricing formula. First, it does not account for the lag in the inflation indexation of the TIPS payoff. The potential error from this omission should be modest (see Grishchenko and Huang 2013), especially as we exclude bonds from our sample when they have less than one year remaining maturity. Second, it neglects the potential deflation protection option in TIPS. TIPS offer some deflation projection because investors are guaranteed the return of their original principal even if the price index declines on net over the life of the bond. This deflation protection option is at the money for every TIPS upon issuance; however, with generally positive inflation since 1997, these options have quickly fallen deeply out of the money and have become of negligible value (see ACR).

Finally, to complete the description of the T-O-L model, we again specify an essentially affine risk premium structure, which implies that the risk premiums Γ_t take the form

$$\Gamma_t = \gamma^0 + \gamma^1 X_t,$$

where $\gamma^0 \in \mathbf{R}^4$ and $\gamma^1 \in \mathbf{R}^{4\times 4}$ contain unrestricted parameters. Thus, the resulting unrestricted four-factor T-O-L model has P-dynamics given by

$$\begin{pmatrix} dL_t \\ dS_t \\ dC_t \\ dX_t^{liq} \end{pmatrix} = \begin{pmatrix} \kappa_{11}^P & \kappa_{12}^P & \kappa_{13}^P & \kappa_{14}^P \\ \kappa_{21}^P & \kappa_{22}^P & \kappa_{23}^P & \kappa_{24}^P \\ \kappa_{31}^P & \kappa_{32}^P & \kappa_{33}^P & \kappa_{34}^P \\ \kappa_{41}^P & \kappa_{42}^P & \kappa_{43}^P & \kappa_{44}^P \end{pmatrix} \left(\begin{pmatrix} \theta_1^P \\ \theta_2^P \\ \theta_3^P \\ \theta_4^P \end{pmatrix} - \begin{pmatrix} L_t \\ S_t \\ C_t \\ X_t^{liq} \end{pmatrix} \right) dt + \Sigma \begin{pmatrix} dW_t^{L,P} \\ dW_t^{S,P} \\ dW_t^{C,P} \\ dW_t^{liq,P} \end{pmatrix}.$$

This is the transition equation in the Kalman filter estimation.

3 The TIPS Data

The U.S. Treasury first issued inflation-indexed securities on February 6, 1997. At the end of our sample in December 30, 2016, the amount of TIPS outstanding had a face value of

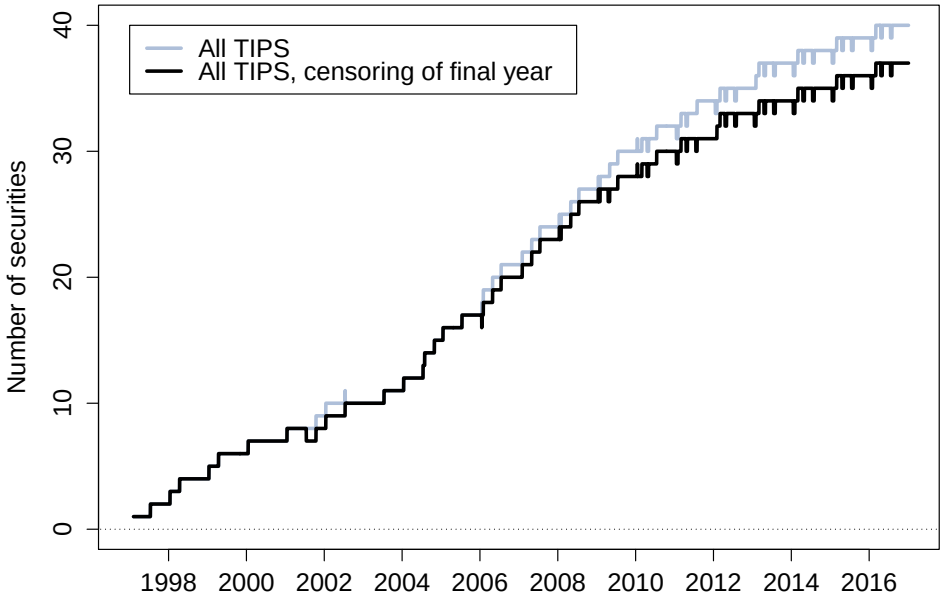

Figure 2: **Number of TIPS Outstanding**

$1.2 trillion, which accounted for about 9 percent of all marketable Treasury debt.[13] The total number of outstanding TIPS over time is shown as a solid gray line in Figure 2. At the end of our sample period—which runs from April 1998 to December 2016—40 TIPS were outstanding. However, as noted by Gürkaynak et al. (2010) and ACR, prices of TIPS near their maturity tend to be somewhat erratic because of the indexation lag in TIPS payouts. Therefore, to facilitate model estimation, we censor TIPS from our sample when they have less than one year to maturity. Using this cutoff, the number of TIPS in the sample is modestly reduced as shown with a solid black line in Figure 2.

The U.S. Treasury has issued ten-year TIPS on a regular basis and five-, twenty-, and thirty-year TIPS more sporadically. The maturity distribution of all 62 TIPS that have been issued since the inception of the indexed-debt program through the end of 2016 is shown in Figure 3. Each TIPS that has been issued is represented by a single downward-sloping line that plots its remaining years to maturity for each date. For the 5- to 10-year maturities of particular interest for our analysis, the universe of TIPS provides fairly good coverage.

[13]The data are available at: http://www.treasurydirect.gov/govt/reports/pd/mspd/2016/opds122016.pdf

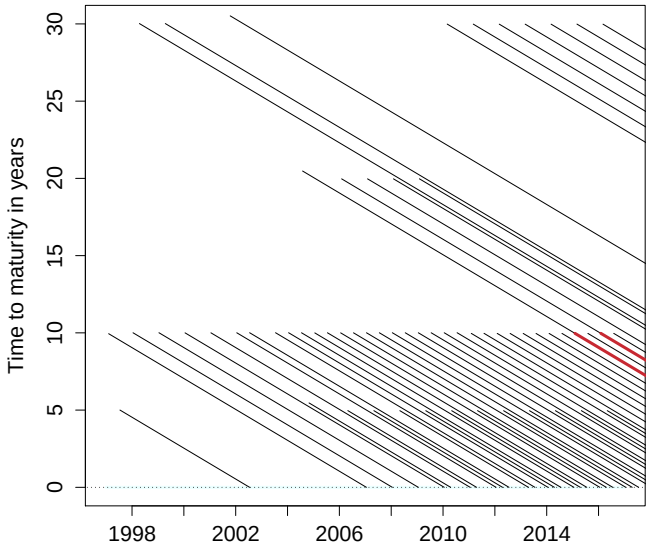

Figure 3: **Maturity Distribution of all TIPS Issued**
The maturity distribution of all TIPS issued is shown by solid black lines. Thick red lines highlight overlapping pairs of recent ten-year and seasoned twenty-year TIPS with identical maturity dates.

4 Estimation of TIPS-only Term Structure Models

In this section, we describe the restrictions imposed to achieve econometric identification of the real term structure models estimated using only TIPS. We then compare estimates of models with and without a liquidity adjustment.

4.1 Econometric Identification

Due to the nonlinearity of the TIPS pricing formula, the models cannot be estimated with the standard Kalman filter. Instead, we use the extended Kalman filter as in Kim and Singleton (2012), see Appendix B for details. To make the fitted errors comparable across TIPS of different maturities, we scale each TIPS price by its duration. Thus, the measurement equation for the TIPS prices takes the following form:

$$\frac{\overline{P}_t(t_0^i, \tau^i, C^i)}{D_t(\tau^i, C^i)} = \frac{\widehat{P}_t(t_0^i, \tau^i, C^i)}{D_t(\tau^i, C^i)} + \varepsilon_t^i,$$

where $\widehat{P}_t(t_0^i, \tau^i, C^i)$ is the model-implied price of TIPS i and $D_t(\tau^i, C^i)$ is its duration, which is fixed and calculated before estimation. We assume that all TIPS measurement errors are $i.i.d.$ with zero mean and standard deviation σ_ε.

K^P	$K^P_{\cdot,1}$	$K^P_{\cdot,2}$	$K^P_{\cdot,3}$	θ^P		Σ
$K^P_{1,\cdot}$	0.2163	-0.0671	-0.0500	0.0349	σ_{11}	0.0045
	(0.1684)	(0.0541)	(0.0511)	(0.0089)		(0.0001)
$K^P_{2,\cdot}$	-0.1839	0.9019	-0.0561	-0.0236	σ_{22}	0.0247
	(1.0568)	(0.3890)	(0.4147)	(0.0074)		(0.0010)
$K^P_{3,\cdot}$	-1.7790	0.4520	1.0854	-0.0183	σ_{33}	0.0281
	(1.1706)	(0.4946)	(0.4860)	(0.0181)		(0.0018)

Table 1: **Estimates of T-O Model**
The table shows the estimated parameters of the K^P matrix, θ^P vector, and diagonal Σ matrix in the T-O model. The estimated value of λ is 0.3849 (0.0032). The maximum log likelihood value is 25,852.69. The numbers in parentheses are the estimated parameter standard deviations.

To identify the four factors of the T-O-L model, we need at least four TIPS securities at each observation date. This requirement implies that the earliest starting point for the model estimation is the issuance date of the fourth TIPS in April 1998.[14] Since the liquidity factor is latent, its level is not identified without additional restrictions. As a consequence, we let the first thirty-year TIPS issued, that is, the TIPS with 3.625% coupon issued on April 15, 1998 with maturity on April 15, 2028, have a unit loading on the liquidity factor, that is, $\beta^i = 1$ for this security. This choice implies that the β^i sensitivity parameters measure liquidity sensitivity relative to that of the thirty-year 2028 TIPS.

Furthermore, we note that the $\lambda^{L,i}$ parameters can be hard to identify if their values are too large or too small. Therefore, we impose the restriction that they fall within the range from 0.0001 to 10. Although binding for a few TIPS, these restrictions are effectively without any practical consequences. Also, for numerical stability during model optimization, we impose the restriction that the β^i parameters fall within the range from 0 to 250, which also turns out not to be a binding constraint at the optimum.

Finally, we note that there does not appear to be any on-the-run premiums in the TIPS market as documented by Christensen et al. (2017), unlike the case in the regular Treasury market. By implication, there are no special price dynamics for individual TIPS following their issuance to take into account.

4.2 Model Estimates

Here we compare the estimated real term structure T-O and T-O-L models to elucidate their dynamics and the effect of the liquidity adjustment. The estimated dynamic parameters of these models are reported in Tables 1 and 2, respectively. We note the usual pattern that the level factor is the most persistent and least volatile factor, the curvature factor is the

[14] Note that for the identification of the T-O model we only need three TIPS to be trading and can start its estimation in January 1998.

K^P	$K^P_{\cdot,1}$	$K^P_{\cdot,2}$	$K^P_{\cdot,3}$	$K^P_{\cdot,4}$	θ^P		Σ
$K^P_{1,\cdot}$	0.2344	-0.1023	-0.0182	0.1395	0.0366	σ_{11}	0.0053
	(0.2795)	(0.0862)	(0.1007)	(0.1800)	(0.0089)		(0.0003)
$K^P_{2,\cdot}$	-1.0889	0.6835	-0.0497	1.5390	-0.0215	σ_{22}	0.0218
	(0.8451)	(0.4735)	(0.5389)	(0.6996)	(0.0161)		(0.0025)
$K^P_{3,\cdot}$	-0.5291	0.2086	1.0451	-0.1062	-0.0227	σ_{33}	0.0281
	(0.8173)	(0.5248)	(0.5333)	(0.6958)	(0.0157)		(0.0033)
$K^P_{4,\cdot}$	-0.8532	0.0859	-0.2464	2.6430	0.0145	σ_{44}	0.0311
	(0.8990)	(0.7395)	(0.8084)	(0.8028)	(0.0070)		(0.0071)

Table 2: **Estimates of the T-O-L Model**
The table shows the estimated parameters of the K^P matrix, θ^P vector, and diagonal Σ matrix in the T-O-L model. The estimated value of λ is 0.4094 (0.0079), while $\kappa^Q_{liq} = 1.0347$ (0.1094) and $\theta^Q_{liq} = 0.0019$ (0.0005). The maximum log likelihood value is 28,574.43. The numbers in parentheses are the estimated parameter standard deviations.

most volatile and least persistent, and the slope factor has dynamic properties in between those two extremes. Finally, the estimated values of λ are about 0.4, which is typical of previous estimates for this parameter using nominal U.S. Treasury data. Thus, in terms of dynamic characteristics for the frictionless factors in the models, the results are very similar to what other studies have reported for nominal Treasury yields using standard Gaussian AFNS models.

The estimated paths of the level, slope, and curvature factors from the two models are shown in Figure 4. The two models' level and curvature factors are fairly close to each other during the entire sample, but there is a notable difference between the two estimated slope factors in the years following the financial crisis. Accordingly, the main impact of accounting for TIPS liquidity premiums is on the slope of the frictionless real yield curve. As we demonstrate later, this affects the models' longer-run projections of real rates and hence the estimates of the natural rate. As for the liquidity factor in the T-O-L model, it is a volatile but quickly mean-reverting process with an estimated mean of 0.0145, which is close to the average of its filtered path shown in Figure 4(d).

The estimated liquidity sensitivity parameters $(\beta^i, \lambda^{L,i})$ for each TIPS in the sample are reported in Appendix C. The estimated values of β^i are mostly in the vicinity of one, but a fair number of TIPS have values much higher to offset the impact of very low values of $\lambda^{L,i}$, which creates a unique shape for their yield sensitivity to the liquidity risk factor as explained in ACR. Appendix C also reports the summary statistics for the fitted errors of each TIPS implied by both the T-O model and the T-O-L model. These errors are calculated by converting the fitted TIPS prices from the model estimation into fitted yields to maturity that are deducted from the mid-market yields to maturity downloaded from Bloomberg. For all TIPS yields combined the RMSE for the T-O model is 8.72 basis points, which is lowered

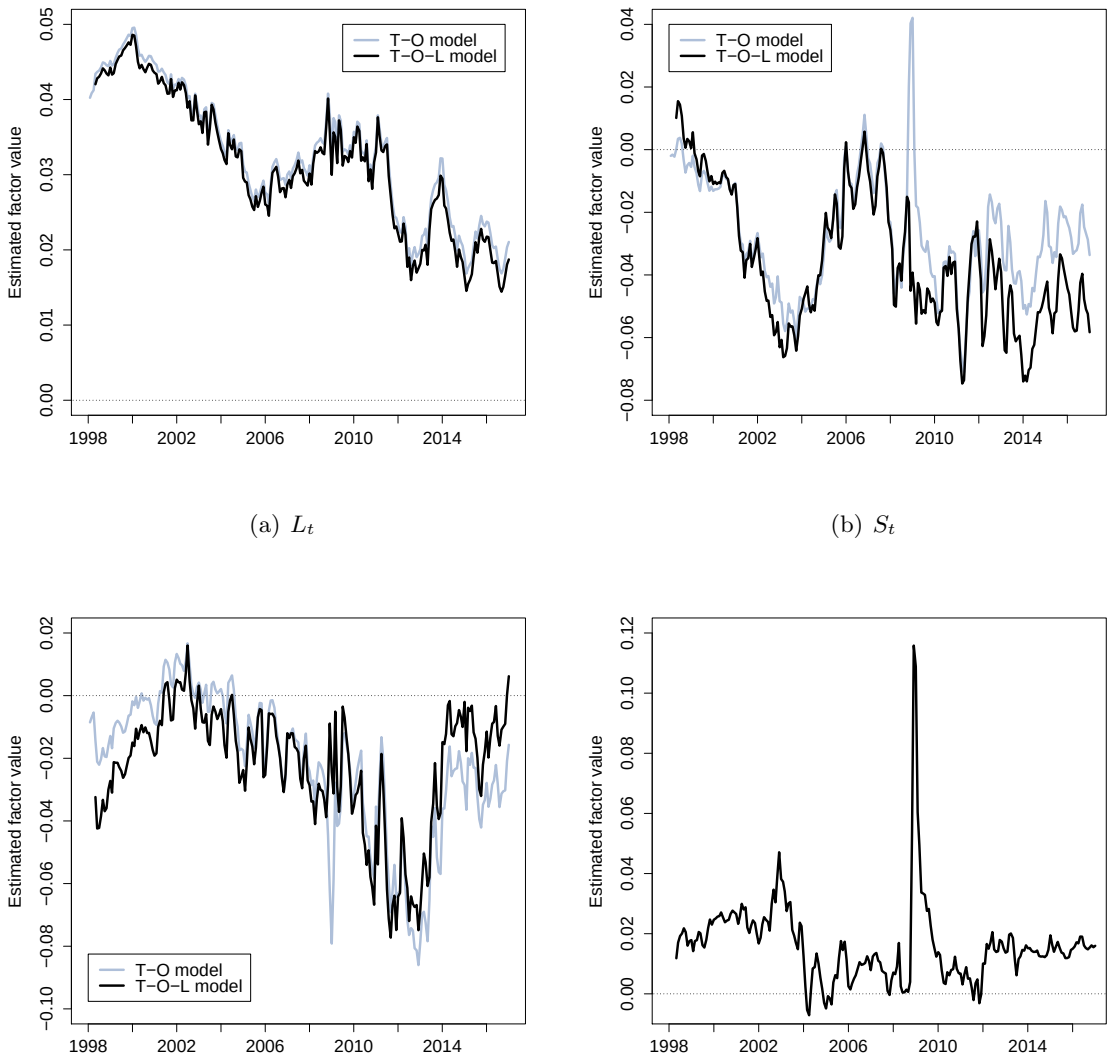

(a) L_t

(b) S_t

(c) C_t

(d) X_t^{liq}

Figure 4: **Estimated State Variables**

Illustration of the estimated state variables from the T-O and T-O-L models. The sample used in the T-O model estimation is monthly covering the period from January 1998 to August 2016, while the sample used in the T-O-L model estimation is monthly covering the period from April 1998 to August 2016.

to 4.31 basis points in the estimation of the T-O-L model, which is about as accurate as in ACR, although they only use five- and ten-year TIPS in their analysis. This suggests that, absent the added computational burden, there is no material loss in model performance from using all available TIPS information. This point is also made by Andreasen, Christensen, and Rudebusch (2017) in the context of Canadian government bond prices.

The average estimated TIPS liquidity premium is 37 basis points, which is similar to

the estimate reported by ACR, although their data are weekly and for a shorter sample. The time series pattern of variation in the premium is also similar in the two models. The average estimated TIPS liquidity premium has been mostly above its historical mean since the financial crisis, which accounts for the wedge between the estimated slope factors from the T-O and T-O-L models observed in Figure 4(b). Furthermore, the relatively stable level of the average liquidity premium implies that it is *not* variation in TIPS liquidity premiums that accounts for the long-term trend lower in real yields. This is important for our analysis as it implies that it must be either declines in expected real rates or their associated term premiums that are behind the decline in real yields the past two decades.

In the asset pricing literature there is much debate about the shape of the real yield curve. Here, we model observed TIPS prices directly with a flexible T-O-L model structure that accommodates level, slope, and curvature patterns in the frictionless part of the TIPS data. Hence, our analysis is imposing a minimum of restrictions on the fundamental or frictionless real yield curve. Yet the estimation results reveal that, for U.S. data, it is indeed the case that the frictionless real yield curve is upward sloping most of the time as also suggested by the observable TIPS yields. This can also be inferred from Figures 4(b) and 4(c) by the fact that the slope and curvature factor within the T-O-L model are almost systematically negative.

5 A Lower New Normal for Interest Rates?

In this section, we use a TIPS-only model that accounts for liquidity and term premiums to obtain expected real short rates and the associated measure of the equilibrium real rate. We then compare this estimate to other market-based and macro-based estimates from the literature and consider the persistence of forces that may be pushing the real rate lower.

5.1 TIPS-only Estimates of the Natural Rate

Our market-based measure of the natural rate is the average expected real short rate over a five-year period starting five years ahead. This 5yr5yr forward average expected real short rate should be little affected by short-term transitory shocks and well positioned to capture the persistent trends in the natural real rate.

Figure 5 shows the T-O-L model decomposition of the 5yr5yr forward frictionless real yield based on equation (2). The solid grey line is the 5yr5yr forward real term premium, which, although volatile, has fluctuated around a fairly stable level since the late 1990s. As suggested by theory, this premium is countercyclical and elevated during economic recessions. In contrast, the estimate of the natural rate of interest implied by the T-O-L model—the black line—shows a gradual decline from just over 2 percent in the late 1990s to about zero by the end of the sample. Importantly, much of the downward trend in 5yr5yr forward real

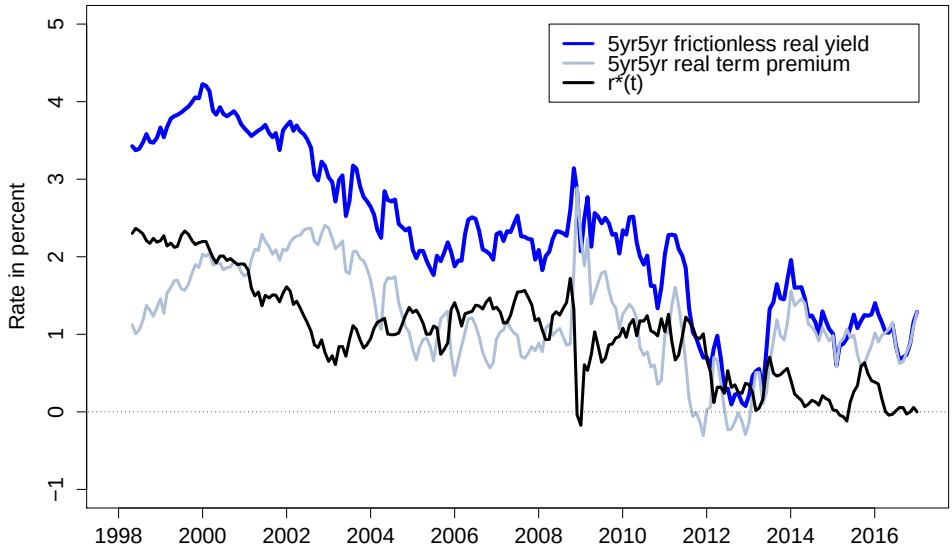

Figure 5: **T-O-L Model 5yr5yr Real Yield Decomposition**

yields is driven by declines in this measure of r_t^*.

The effect on the estimated natural rate from accounting for liquidity premiums in TIPS prices is the subject of Figure 6. The black line is the estimate of r_t^* from the T-O-L model, and the grey line is the estimate from the T-O model, which does not account for time-varying liquidity effects in TIPS prices. Accounting for the liquidity premiums in TIPS prices leads to notable differences in the natural rate estimate at times, and the mean absolute difference between the two estimates is 27 basis points over the sample. Still, the general magnitude and timing of the overall downtrend in the natural interest rate is similar across the two specifications.

5.2 Comparison of Estimates of the Natural Rate

There are a variety of other estimates of the equilibrium or natural interest rate in the literature that can be compared to our TIPS-only estimates. To start, we compare the r_t^* estimates from the T-O-L model to two other estimates that employ financial models and bond market data. Specifically, we consider the joint models of nominal and real yields developed by Abrahams et al. (2016, henceforth AACMY) and ACR. Both of these models adjust for term and liquidity premiums in TIPS yields, so they are obvious benchmarks for

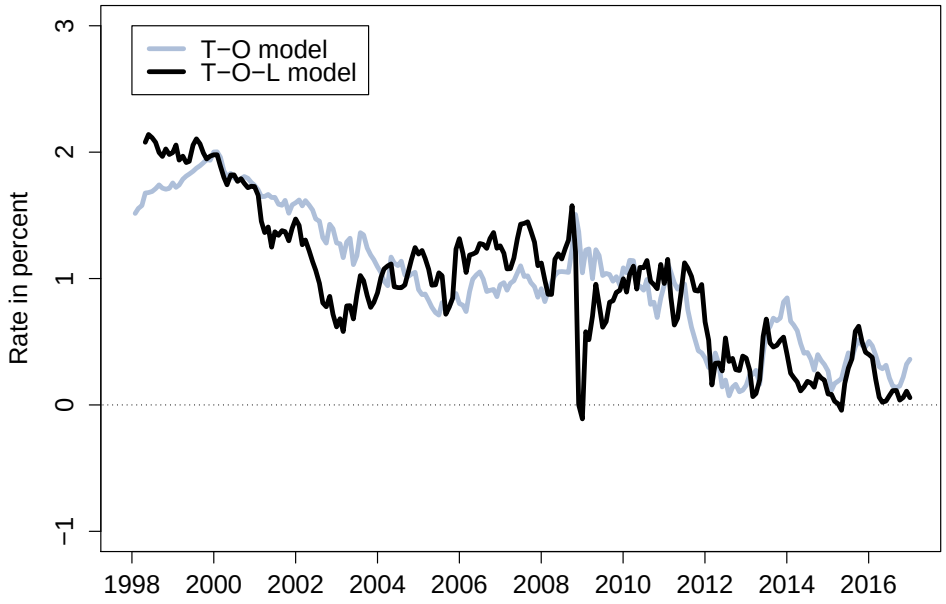

Figure 6: **Effect of Liquidity Adjustment on Estimates of r***

comparison. All three market-based estimates of the natural rate are shown in Figure 7.[15] The ACR model provides r_t^* estimates that are only a bit lower than the T-O-L model on average though they are more cyclically variable. By contrast, the AACMY model has an r_t^* estimate below zero for almost the entire sample and is a clear outlier in this comparison and relative to the broader literature on natural rate estimates.

Since the very different AACMY and ACR estimates both come from joint representations of nominal and real yields, that modeling attribute does not seem to be the crucial determinant of the natural rate estimates. Instead, to understand and explain the dispersion in the estimates, a few key differences in model specification are worth highlighting. The T-O-L model has a four-factor structure and exploits price information for all TIPS—including twenty- and thirty-year maturities. ACR use a five-factor structure that imposes restrictions between the slope and curvature of the nominal yield curve and those of the real yield curve first detailed in Christensen et al. (2010). In contrast, AACMY use a very flexible six-factor model of nominal and real yields with two separate TIPS-specific factors. As a consequence, the model provides very tight in-sample fit to the observed yields, but that flexibility may

[15] A very different perspective is provided by Kaminska and Zinna (2014), who estimate a no-arbitrage model of TIPS using official foreign and Fed bond demand as a pricing factor. They find steep cyclically-insensitive declines over the past two decades in the long-run real term premium—from 2 to -2 percent—and relatively stable expected future short rates.

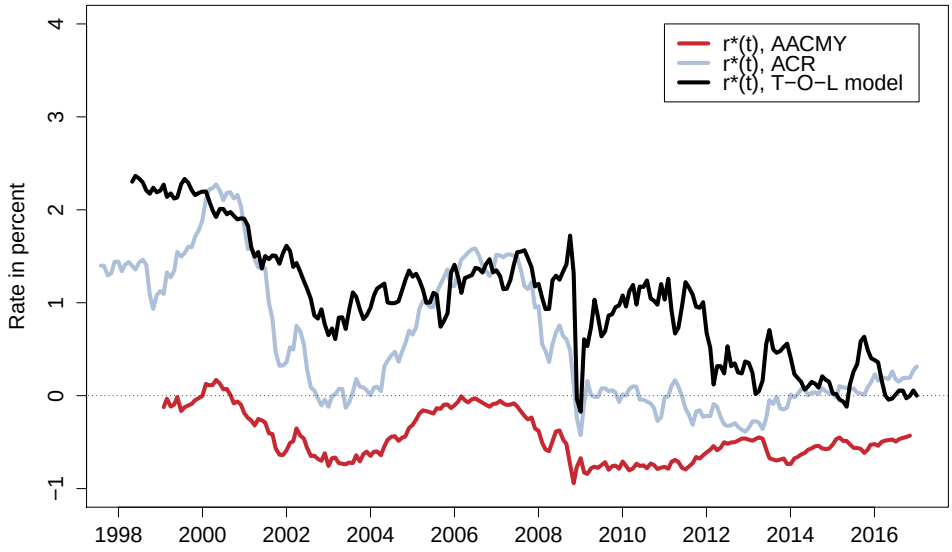

Figure 7: **Comparison with Market-Based Estimates of r***

come at the cost of over-fitting and delivering less accurate estimates of the factor P-dynamics. Since those dynamics are critical to the model-implied estimates of r_t^*, as evident in equation (1), this may explain the unusually low AACMY estimates of r_t^*. In addition, the AACMY model only uses yields with maturities up to ten years, which may compound problems with the estimation of the factor dynamics as their sample is dominated by short- and medium-term yields that have a tendency to revert back to mean at a quicker pace than long-term yields. The reduced variance of the AACMY estimates of r_t^* during the period when nominal rates were constrained by the zero lower bound also seems to be problematic.

These three theoretically consistent arbitrage-free models can also deliver estimates of the term premium, which provide another dimension for comparison. Figure 8 shows the 5yr5yr real term premium estimates from AACMY, ACR, and the T-O-L model. The real term premium estimates from ACR and the T-O-L model match remarkably closely showing countercyclical fluctuations around what looks to be a steady mean. In contrast, the real term premium estimate from AACMY drifts lower over the sample, which could be another sign that its factor dynamics are not sufficiently persistent and potentially plagued by finite-sample bias problems as discussed in detail in Bauer et al. (2012).

To further evaluate the r_t^* estimate from the T-O-L model, we now turn to estimates obtained from macroeconomic models and data. Figure 9 provides a comparison with macro-based estimates of r^*, that is, estimates derived from macroeconomic models and data. The

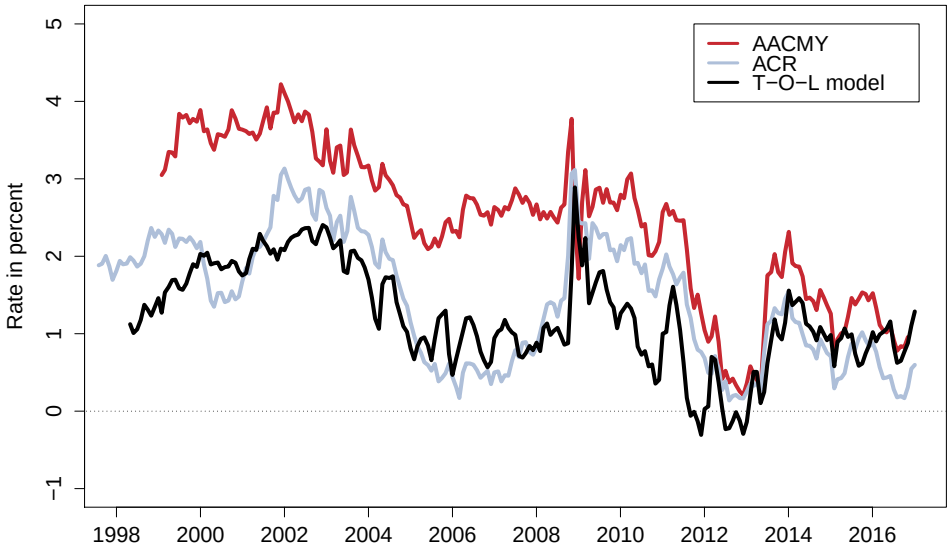

Figure 8: **Estimates of the 5yr5yr Real Yield Term Premium**

specific series shown—the grey line—is a composite macro-based measure that averages across three fairly similar macro-based estimates.[16] The black line shows our preferred TIPS-only estimate of r_t^*. The macro-based estimate shown in the figure starts in 1980–almost 20 years earlier than the TIPS-only estimate. However, in the 1980s and 1990s, the macro-based estimate changes little and remains close to 2-1/2 percent the whole time. This is consistent with the received wisdom of that era in monetary economics that viewed the natural rate as effectively constant—for example, as assumed in the large Taylor rule literature. It is only in the late 1990s that a decided downtrend begins in the macro-based r_t^* estimates. This decline starts about the same time as when TIPS are introduced which is quite a fortuitous coincidence for our purposes. Accordingly, even though our estimation sample is limited to the past two decades, the evidence suggests that this is the precise sample of most relevance for discerning shifts in the equilibrium real rate.

During their shared sample, the macro-based and T-O-L model estimates exhibit a similar general trend—starting from just above 2 percent in the late 1990s and ending the sample near zero. There are, however, important differences in timing between the two estimates.[17]

[16] Specifically, the macro-based composite is the average of the filtered estimate from Laubach and Williams (2016), the filtered mean estimate from Johannsen and Mertens (2016), and the estimated median from Lubick and Matthes (2015). The averaging smoothes across the specific modeling assumptions in the different empirical representations in these studies.

[17] It should be noted that the TIPS-based natural rate estimates use the CPI as the price index, but the macro-based estimates use an alternative price deflator for personal consumption expenditures, which would

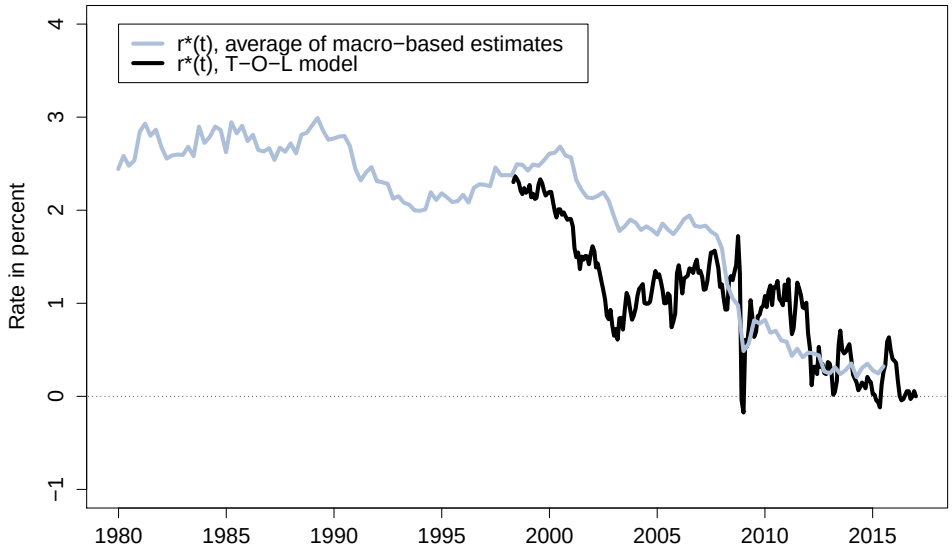

Figure 9: **Comparison with Macro-Based Estimates of r***

The macro-based estimate of the natural rate shows only a modest decline from the late 1990s until the financial crisis and the start of the Great Recession. Then, it drops precipitously to less than 1 percent and edges only slightly lower thereafter. The TIPS-only estimate instead declines in the early 2000s, stabilizes, and then declines a bit more in 2012. Both methodologies imply that r_t^* is currently near its historical low.

Finally, Figure 10 compares the T-O-L model r_t^* to estimates of the natural real rate implied in the long-run forecasts from the Blue Chip Financial Forecasts survey of professional forecasters and from the Congressional Budget Office (CBO). The Blue Chip and CBO natural rate estimates are obtained by subtracting 5- to 10-year ahead projected CPI inflation from the projected three-month Treasury bill rate at a similar horizon. Note that the r_t^* estimate from the T-O-L model is highly positively correlated with the r_t^* estimate implied by the Blue Chip survey with the same notable decline in the early 2000s. The CBO's estimate changes little for much of the early sample, but like the other r_t^* series, it also exhibits a clear downtrend later on.

5.3 Projections of the Natural Rate

In light of the intense debate among researchers, investors, and policymakers about whether there is a new lower normal for interest rates, we end our analysis by presenting the outlook

lead to higher estimates of the natural real rate on average by around 30 basis points.

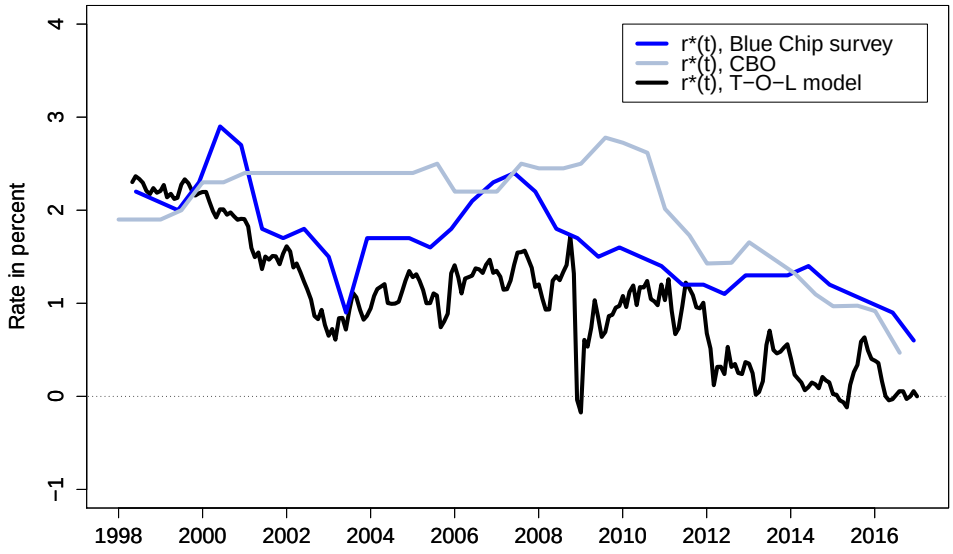

Figure 10: **Comparison with Blue Chip and CBO Estimates of r***

for the natural rate based on the T-O-L model. We follow the approach of Christensen et al. (2015) and simulate 10,000 factor paths over a ten-year horizon conditioned on the shape of the TIPS yield curve and investors' embedded forward-looking expectations as of the end of our sample (that is, using estimated state variables and factor dynamics as of December 30, 2016). The simulated factor paths are then converted into forecasts of r_t^*. Figure 11 shows the median projection and the 5th and 95th percentile values for the simulated natural rate over a ten-year forecast horizon.[18]

The median r_t^* projection shows only a very gradual partial reversal of the declines the past two decades and only reaches 1 percent by 2025. The upper 95th percentile rises more rapidly while the lower 5th percentile represents outcomes with the natural rate trending persistently lower into negative territory and remaining there over the entire forecast horizon. The underlying stationarity of the T-O-L model is clear in these conditional forecasts. Of course, like most estimates of persistent dynamics, the model will likely suffer from some finite-sample bias in the estimated parameters of its mean-reversion matrix K^P, which would imply that it does not exhibit a sufficient amount of persistence—as described in Bauer et al. (2012). In turn, this would suggest (all else equal) that the outcomes below the median are more likely than a straight read of the simulated probabilities indicate, and correspondingly those above

[18]Note that the lines do not represent short rate paths from a single simulation run over the forecast horizon; instead, they delineate the distribution of all simulation outcomes at a given point in time.

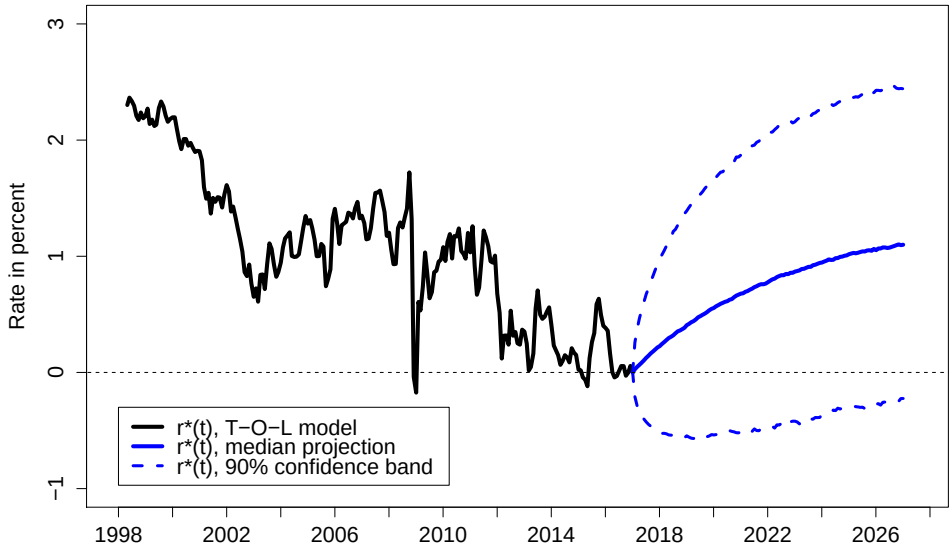

Figure 11: **Ten-Year Projections of r* from T-O-L Model**

the median are less likely than indicated. As a consequence, we view the projections in Figure 11 as an upper bound estimate of the true probability distribution of the future path for the natural rate. As a result, we consider it even more likely that the natural rate will remain at or near its current new low for the foreseeable future.

Finally, we believe that our time series estimate of r_t^* is relevant to the debate about the source of the decline in the equilibrium real rate. In particular, although our measure of the real rate fluctuated a bit at the start of the Financial Crisis, our average r_t^* estimate in 2010 and 2011 is not much different than in 2006 and 2007. This relative stability before and after the Financial Crisis suggests that flight-to-safety and safety premium explanations of the lower equilibrium real rate are unlikely to be key drivers of the downtrend in Treasury rates (as proposed by Hall 2016 among others). Instead, our estimates appear more broadly consistent with many of the explanations that attribute the decline in the natural rate to real-side fundamentals such as changing demographics (e.g., Carvalho et al. 2016, Favero et al. 2016, and Gagnon et al. 2016).

6 Conclusion

Given the historic downtrend in yields in recent decades, many researchers have investigated the factors pushing down the steady-state level of the safe short-term real interest rate.

However, all of this empirical work has been based on *macroeconomic* models and data. To complement this analysis, we examine the dynamics of the equilibrium real rate using dynamic term structure models estimated solely on the prices of inflation-indexed bonds. By adjusting for both TIPS liquidity premiums and real term premiums, we uncover investors' expectations for the underlying frictionless real short rate for the five-year period starting five years ahead. This measure of the natural rate of interest exhibits a gradual decline over the past two decades that accounts for about half of the general decline in yields. Specifically, as of the end of December 2016, the T-O-L model r_t^* estimate is essentially zero, a decline of around 2-1/4 percentage points since the beginning of 1998. Furthermore, model projections that exploit the estimated factor dynamics suggest that this measure of the natural rate is more likely than not to remain near its current low for the foreseeable future.

Given that our measure of the natural rate of interest is based on the forward-looking information priced into an active TIPS market and can be updated at daily frequency, it could serve as an important input for real-time monetary policy analysis. For future research, our methods could also be expanded along an international dimension. With a significant degree of capital mobility, the natural rate will depend on global saving and investment, so the joint modeling of inflation-indexed bonds in several countries could be informative (see Holston, Laubach, and Williams 2017 for an international discussion of the natural rate). Finally, our measure could be incorporated into an expanded joint macroeconomic and finance model analysis—particularly with an eye towards further understanding the determinants of the lower new normal for interest rates.

Appendix A: Analytical TIPS Pricing Formula

In this appendix, we provide the analytical formula for the price of individual TIPS within the T-O-L model described in Section 2.3. The net present value of one unit of the consumption basket paid at time $t+\tau$ by TIPS i with liquidity sensitivity parameter, β^i, and liquidity decay parameter, $\lambda^{L,i}$, can be calculated by the formula provided in the following proposition. (Details are available upon request.)

Proposition 1:

The net present value of one unit of the consumption basket paid at time $t+\tau$ by TIPS i with liquidity sensitivity parameter, β^i, and liquidity decay parameter, $\lambda^{L,i}$, is given by

$$\begin{aligned} P^i(t_0^i,t,T) &= E_t^Q\Big[e^{-\int_t^T (r_s+\beta^i(1-e^{-\lambda^{L,i}(s-t_0^i)})X_s^{Liq})ds}e^{(\overline{B}^i)'X_T+\overline{A}^i}\Big] \\ &= \exp\Big(B_1^i(t,T)L_t+B_2^i(t,T)S_t+B_3^i(t,T)C_t+B_4^i(t_0^i,t,T)X_t^{Liq}+A^i(t_0^i,t,T)\Big), \end{aligned}$$

where

$$\begin{aligned} B_1^i(t,T) &= \overline{B}_1^i-(T-t), \\ B_2^i(t,T) &= e^{-\lambda(T-t)}\overline{B}_2^i-\frac{1-e^{-\lambda(T-t)}}{\lambda}, \\ B_3^i(t,T) &= \lambda(T-t)e^{-\lambda(T-t)}\overline{B}_2^i+\overline{B}_3^i e^{-\lambda(T-t)}+\Big[(T-t)e^{-\lambda(T-t)}-\frac{1-e^{-\lambda(T-t)}}{\lambda}\Big], \\ B_4^i(t_0^i,t,T) &= e^{-\kappa_{Liq}^Q(T-t)}\overline{B}_4^i-\beta^i\frac{1-e^{-\kappa_{Liq}^Q(T-t)}}{\kappa_{Liq}^Q}+\beta^i e^{-\lambda^{L,i}(t-t_0^i)}\frac{1-e^{-(\kappa_{Liq}^Q+\lambda^{L,i})(T-t)}}{\kappa_{Liq}^Q+\lambda^{L,i}}, \\ A^i(t_0^i,t,T) &= \overline{A}^i-\beta^i\theta_{liq}^Q(T-t)+\theta_{liq}^Q\Big[\overline{B}_5^i+\frac{\beta^i}{\kappa_{Liq}^Q}-\beta^i\frac{e^{-\lambda^{L,i}(T-t_0^i)}}{\kappa_{Liq}^Q+\lambda^{L,i}}\Big](1-e^{-\kappa_{Liq}^Q(T-t)}) \\ &\quad+\beta^i\frac{\kappa_{liq}^Q\theta_{liq}^Q}{\kappa_{Liq}^Q+\lambda^{L,i}}\frac{e^{-\lambda^{L,i}(t-t_0^i)}-e^{-\lambda^{L,i}(T-t_0^i)}}{\lambda^{L,i}}+\frac{\sigma_{11}^2}{6}[(\overline{B}_1^i)^3-(\overline{B}_1^i-(T-t))^3] \\ &\quad+\sigma_{22}^2\Big[\frac{1}{2\lambda^2}(T-t)-\frac{(1+\lambda\overline{B}_2^i)}{\lambda^3}[1-e^{-\lambda(T-t)}]+\frac{(1+\lambda\overline{B}_2^i)^2}{4\lambda^3}[1-e^{-2\lambda(T-t)}]\Big] \\ &\quad+\sigma_{33}^2\Bigg[\frac{1}{2\lambda^2}(T-t)+\frac{1+\lambda\overline{B}_2^i}{\lambda^2}(T-t)e^{-\lambda(T-t)}-\frac{(1+\lambda\overline{B}_2^i)^2}{4\lambda}(T-t)^2e^{-2\lambda(T-t)} \\ &\qquad-\frac{(1+\lambda\overline{B}_2^i)(3+\lambda\overline{B}_2^i+2\lambda\overline{B}_3^i)}{4\lambda^2}(T-t)e^{-2\lambda(T-t)} \\ &\qquad+\frac{(2+\lambda\overline{B}_2^i+\lambda\overline{B}_3^i)^2+(1+\lambda\overline{B}_3^i)^2}{8\lambda^3}[1-e^{-2\lambda(T-t)}]-\frac{2+\lambda\overline{B}_2^i+\lambda\overline{B}_3^i}{\lambda^3}[1-e^{-\lambda(T-t)}]\Bigg] \\ &\quad+\frac{\sigma_{44}^2}{2}\Bigg[\frac{(\beta^i)^2}{(\kappa_{Liq}^Q)^2}(T-t)+\Big[\overline{B}_5^i+\frac{\beta^i}{\kappa_{Liq}^Q}-\beta^i\frac{e^{-\lambda^{L,i}(T-t_0^i)}}{\kappa_{Liq}^Q+\lambda^{L,i}}\Big]^2\frac{1-e^{-2\kappa_{Liq}^Q(T-t)}}{2\kappa_{Liq}^Q} \\ &\qquad+\frac{(\beta^i)^2}{(\kappa_{Liq}^Q+\lambda^{L,i})^2}\frac{e^{-2\lambda^{L,i}(t-t_0^i)}-e^{-2\lambda^{L,i}(T-t_0^i)}}{2\lambda^{L,i}}-2\frac{\beta^i}{\kappa_{Liq}^Q}\Big[\overline{B}_5^i+\frac{\beta^i}{\kappa_{Liq}^Q}-\beta^i\frac{e^{-\lambda^{L,i}(T-t_0^i)}}{\kappa_{Liq}^Q+\lambda^{L,i}}\Big]\frac{1-e^{-\kappa_{Liq}^Q(T-t)}}{\kappa_{Liq}^Q} \\ &\qquad-2(\beta^i)^2\frac{1}{\kappa_{Liq}^Q}\frac{1}{\kappa_{Liq}^Q+\lambda^{L,i}}\frac{e^{-\lambda^{L,i}(t-t_0^i)}-e^{-\lambda^{L,i}(T-t_0^i)}}{\lambda^{L,i}} \\ &\qquad+2\beta^i\Big[\overline{B}_5^i+\frac{\beta^i}{\kappa_{Liq}^Q}-\beta^i\frac{e^{-\lambda^{L,i}(T-t_0^i)}}{\kappa_{Liq}^Q+\lambda^{L,i}}\Big]e^{-\lambda^{L,i}(t-t_0^i)}\frac{e^{-\lambda^{L,i}(T-t)}-e^{-\kappa_{Liq}^Q(T-t)}}{(\kappa_{Liq}^Q)^2-(\lambda^{L,i})^2}\Bigg]. \end{aligned}$$

Appendix B: The Extended Kalman Filter Estimation

In this appendix, we describe the estimation of the T-O and T-O-L models based on the extended Kalman filter. For affine Gaussian models, in general, the conditional mean vector and the conditional covariance matrix are[19]

$$\begin{aligned} E^P[X_T|\mathcal{F}_t] &= (I - \exp(-K^P\Delta t))\theta^P + \exp(-K^P\Delta t)X_t, \\ V^P[X_T|\mathcal{F}_t] &= \int_0^{\Delta t} e^{-K^P s}\Sigma\Sigma' e^{-(K^P)' s} ds, \end{aligned}$$

where $\Delta t = T - t$. Conditional moments of discrete observations are computed and the state transition equation is obtained as

$$X_t = (I - \exp(-K^P\Delta t))\theta^P + \exp(-K^P\Delta t)X_{t-1} + \xi_t,$$

where Δt is the time between observations.

In the standard Kalman filter, the measurement equation is linear

$$y_t = A + BX_t + \varepsilon_t$$

and the assumed error structure is

$$\begin{pmatrix} \xi_t \\ \varepsilon_t \end{pmatrix} \sim N\left[\begin{pmatrix} 0 \\ 0 \end{pmatrix}, \begin{pmatrix} Q & 0 \\ 0 & H \end{pmatrix}\right],$$

where the matrix H is assumed to be diagonal, while the matrix Q has the following structure

$$Q = \int_0^{\Delta t} e^{-K^P s}\Sigma\Sigma' e^{-(K^P)' s} ds.$$

In addition, the transition and measurement errors are assumed to be orthogonal to the initial state.

Now consider Kalman filtering, which is used to evaluate the likelihood function. Due to the assumed stationarity, the filter is initialized at the unconditional mean and variance of the state variables under the P-measure: $X_0 = \theta^P$ and $\Sigma_0 = \int_0^\infty e^{-K^P s}\Sigma\Sigma' e^{-(K^P)' s} ds$. Denote the information available at time t by $Y_t = (y_1, y_2, \ldots, y_t)$, and denote model parameters by ψ. Consider period $t-1$ and suppose that the state update X_{t-1} and its mean square error matrix Σ_{t-1} have been obtained. The prediction step is

$$X_{t|t-1} = E^P[X_t|Y_{t-1}] = \Phi_t^{X,0}(\psi) + \Phi_t^{X,1}(\psi)X_{t-1},$$

$$\Sigma_{t|t-1} = \Phi_t^{X,1}(\psi)\Sigma_{t-1}\Phi_t^{X,1}(\psi)' + Q_t(\psi),$$

where $\Phi_t^{X,0} = (I - \exp(-K^P\Delta t))\theta^P$, $\Phi_t^{X,1} = \exp(-K^P\Delta t)$, and $Q_t = \int_0^{\Delta t} e^{-K^P s}\Sigma\Sigma' e^{-(K^P)' s} ds$, while Δt is the time between observations.

In the time-t update step, $X_{t|t-1}$ is improved by using the additional information contained in Y_t:

$$X_t = E[X_t|Y_t] = X_{t|t-1} + \Sigma_{t|t-1}B(\psi)' F_t^{-1} v_t,$$

$$\Sigma_t = \Sigma_{t|t-1} - \Sigma_{t|t-1}B(\psi)' F_t^{-1} B(\psi)\Sigma_{t|t-1},$$

where

$$v_t = y_t - E[y_t|Y_{t-1}] = y_t - A(\psi) - B(\psi)X_{t|t-1},$$

[19] Throughout conditional and unconditional covariance matrices are calculated using the analytical solutions provided in Fisher and Gilles (1996).

$$F_t = cov(v_t) = B(\psi)\Sigma_{t|t-1}B(\psi)' + H(\psi),$$
$$H(\psi) = diag(\sigma_\varepsilon^2(\tau_1), \ldots, \sigma_\varepsilon^2(\tau_N)).$$

At this point, the Kalman filter has delivered all ingredients needed to evaluate the Gaussian log likelihood, the prediction-error decomposition of which is

$$\log l(y_1, \ldots, y_T; \psi) = \sum_{t=1}^{T} \Big(-\frac{N}{2}\log(2\pi) - \frac{1}{2}\log|F_t| - \frac{1}{2}v_t' F_t^{-1} v_t \Big),$$

where N is the number of observed yields. Now, the likelihood is numerically maximized with respect to ψ using the Nelder-Mead simplex algorithm. Upon convergence, the standard errors are obtained from the estimated covariance matrix,

$$\widehat{\Omega}(\widehat{\psi}) = \frac{1}{T}\Big[\frac{1}{T}\sum_{t=1}^{T} \frac{\partial \log l_t(\widehat{\psi})}{\partial \psi} \frac{\partial \log l_t(\widehat{\psi})}{\partial \psi}'\Big]^{-1},$$

where $\widehat{\psi}$ denotes the estimated model parameters.

In the T-O and T-O-L models, the extended Kalman filter is needed because the measurement equations are no longer affine functions of the state variables. Instead, the measurement equation takes the general form

$$\frac{\overline{P}_t^i(t_0^i, \tau^i)}{D_t^i(t_0^i, \tau^i)} = z(X_t; t_0^i, \tau^i, \psi) + \varepsilon_t^i.$$

In the extended Kalman filter, this equation is linearized using a first-order Taylor expansion around the best guess of X_t in the prediction step of the Kalman filter algorithm. Thus, in the notation introduced above, this best guess is denoted $X_{t|t-1}$ and the approximation is given by

$$z(X_t; t_0^i, \tau^i, \psi) \approx z(X_{t|t-1}; t_0^i, \tau^i, \psi) + \frac{\partial z(X_t; t_0^i, \tau^i, \psi)}{\partial X_t}\Big|_{X_t = X_{t|t-1}} (X_t - X_{t|t-1}).$$

Thus, by defining

$$A_t(\psi) \equiv z(X_{t|t-1}; t_0^i, \tau^i, \psi) - \frac{\partial z(X_t; t_0^i, \tau^i, \psi)}{\partial X_t}\Big|_{X_t = X_{t|t-1}} X_{t|t-1} \quad \text{and} \quad B_t(\psi) \equiv \frac{\partial z(X_t; t_0^i, \tau^i, \psi)}{\partial X_t}\Big|_{X_t = X_{t|t-1}},$$

the measurement equation can be given on an affine form as

$$\frac{\overline{P}_t^i(t_0^i, \tau^i)}{D_t^i(t_0^i, \tau^i)} = A_t(\psi) + B_t(\psi)X_t + \varepsilon_t^i$$

and the steps in the algorithm proceed as previously described.

Appendix C: Details of TIPS-Specific Liquidity Estimates

The liquidity factor loadings of individual TIPS zero-coupon discount functions are given by

$$-\frac{B_4(t, t_0^i, \tau)}{\tau} = \beta^i \frac{1 - e^{-\kappa_{Liq}^Q (T-t)}}{\kappa_{Liq}^Q \tau} - \beta^i e^{-\lambda^{L,i}(t - t_0^i)} \frac{1 - e^{-(\kappa_{Liq}^Q + \lambda^{L,i})(T-t)}}{(\kappa_{Liq}^Q + \lambda^{L,i})\tau}.$$

With β^i set to 1, the loadings as a function of time since issuance are shown in Figure 12. For small $\lambda^{L,i}$, the loading approximates a level factor, while high $\lambda^{L,i}$ (0.25 and above) produce a classic slope factor pattern. In the latter case, the idiosyncratic bond-specific variation tied to how much of the security is locked up in buy-and-hold portfolios is dwarfed by expectations about the systematic risk that variation in X_t^{liq} represents.

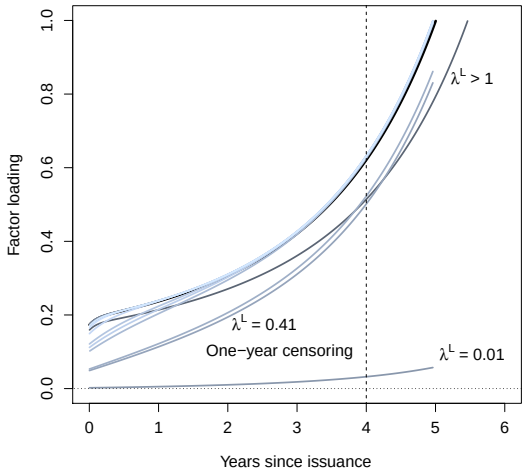

(a) Five-year TIPS

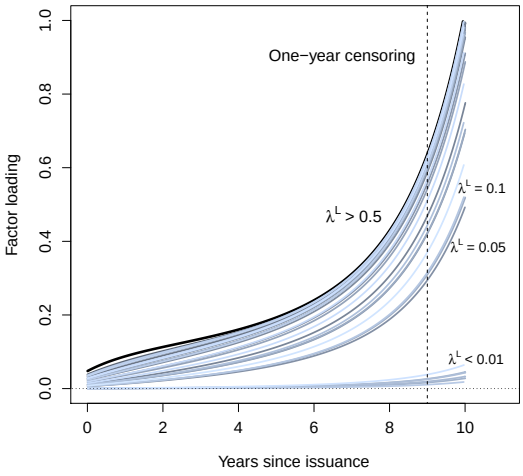

(b) Ten-year TIPS

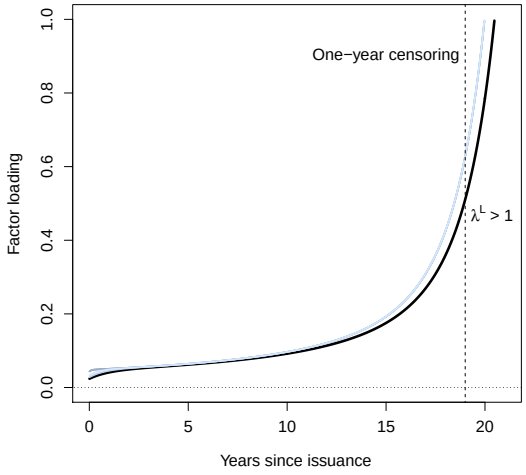

(c) Twenty-year TIPS

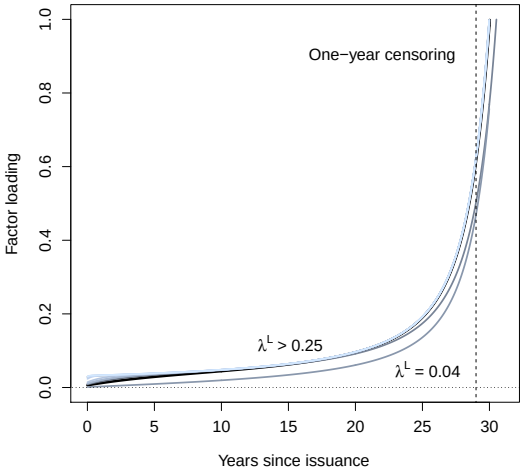

(d) Thirty-year TIPS

Figure 12: **Factor Loadings of the Liquidity Factor**

Factor loadings of the liquidity factor in individual TIPS zero-coupon bond yield functions as a function of the time since issuance, that is, $\frac{1-e^{-\kappa^Q_{Liq}(T-t)}}{\kappa^Q_{Liq}(T-t)} - e^{-\lambda^{L,i}(t-t^i_0)}\frac{1-e^{-(\kappa^Q_{Liq}+\lambda^{L,i})(T-t)}}{(\kappa^Q_{Liq}+\lambda^{L,i})(T-t)}$.

Estimated liquidity sensitivity parameters and model fit for each TIPS are given in Table 3. The table also reports the number of monthly observations for each TIPS used in the estimation of the T-O-L model.

TIPS (coupon, maturity date)	obs.	T-O-L model						T-O model	
		β^i	Std	$\lambda^{L,i}$	Std	Mean	RMSE	Mean	RMSE
(1) 3.375% 1/15/2007	93	0.70	0.14	1.004	0.843	2.16	4.31	2.14	5.70
(2) 3.625% 7/15/2002*	39	0.27	0.29	9.746	1.496	3.03	3.74	3.11	4.42
(3) 3.625% 1/15/2008	105	0.88	0.16	0.408	0.186	1.67	3.90	2.57	4.73
(4) 3.625% 4/15/2028+	225	1	n.a.	0.239	0.300	2.08	3.88	5.28	6.56
(5) 3.875% 1/15/2009	108	0.88	0.14	0.590	0.335	1.49	3.03	1.98	4.10
(6) 3.875% 4/15/2029+	213	0.96	0.21	0.371	0.611	1.82	3.55	4.60	5.95
(7) 4.25% 1/15/2010	108	0.94	0.15	0.688	0.342	0.33	5.58	1.43	6.57
(8) 3.5% 1/15/2011	108	1.00	0.15	0.553	0.240	-0.20	6.42	-0.10	5.81
(9) 3.375% 4/15/2032+	183	0.57	0.14	9.998	0.952	1.09	4.14	-4.04	6.56
(10) 3.375% 1/15/2012	108	1.05	0.14	0.488	0.275	0.40	3.89	-0.04	3.84
(11) 3% 7/15/2012	108	1.04	0.14	0.584	0.321	-0.56	6.22	-1.55	6.83
(12) 1.875% 7/15/2013	108	1.09	0.14	0.632	0.398	-0.30	5.77	-1.72	9.62
(13) 2% 1/15/2014	108	1.97	0.50	0.151	0.080	1.17	3.39	4.65	8.87
(14) 2% 7/15/2014	108	1.41	0.24	0.315	0.173	0.23	3.45	-0.37	11.62
(15) 2.375% 1/15/2025†	150	0.96	0.18	1.066	0.927	0.79	3.62	3.73	5.64
(16) 0.875% 4/15/2010*	54	1.02	0.15	9.988	0.887	3.73	5.69	7.77	13.54
(17) 1.625% 1/15/2015	108	4.01	0.87	0.068	0.023	0.76	4.14	7.70	11.40
(18) 1.875% 7/15/2015	108	1.73	0.28	0.245	0.091	-0.3	4.72	-0.01	11.16
(19) 2% 1/15/2016	108	2.81	0.69	0.120	0.053	0.56	4.35	6.49	9.90
(20) 2% 1/15/2026†	132	0.87	0.18	9.745	0.849	0.86	3.38	2.40	4.58
(21) 2.375% 4/15/2011*	48	0.98	0.14	10.000	0.985	5.29	12.78	3.40	13.95
(22) 2.5% 7/15/2016	108	1.43	0.18	0.400	0.193	-0.14	4.66	-4.01	13.26
(23) 2.375% 1/15/2017	108	1.96	0.34	0.221	0.101	0.69	4.66	3.39	6.94
(24) 2.375% 1/15/2027†	120	0.83	0.23	9.975	0.857	0.92	2.74	1.56	3.58
(25) 2% 4/15/2012*	48	0.94	0.13	9.997	0.906	6.70	11.25	-0.14	15.16
(26) 2.625% 7/15/2017	108	1.40	0.27	0.352	0.223	-0.05	3.44	-7.87	13.50
(27) 1.625% 1/15/2018	108	2.63	0.88	0.123	0.070	-0.12	4.12	0.20	5.21
(28) 1.75% 1/15/2028†	108	0.70	0.24	1.414	0.923	0.48	2.49	-1.42	3.44
(29) 0.625% 4/15/2013*	48	26.53	0.89	0.012	0.002	2.37	8.44	-14.09	35.60
(30) 1.375% 7/15/2018	102	3.11	0.90	0.074	0.031	-0.36	4.59	-10.17	13.25
(31) 2.125% 1/15/2019	96	76.32	1.43	0.003	0.000	0.53	3.93	0.15	7.70
(32) 2.5% 1/15/2029†	96	0.73	0.27	2.182	1.464	0.34	2.02	-1.07	2.43
(33) 1.25% 4/15/2014*	48	2.15	0.57	0.359	0.202	0.23	4.20	0.27	10.27
(34) 1.875% 7/15/2019	90	40.79	1.41	0.005	0.001	-0.07	2.95	-5.66	7.52
(35) 1.375% 1/15/2020	84	71.02	1.48	0.003	0.001	0.18	2.71	3.32	6.03
(36) 2.125% 2/15/2040+	83	6.52	1.49	0.048	0.027	0.32	3.41	1.05	4.62
(37) 0.5% 4/15/2015*	48	2.50	0.69	0.400	0.216	-0.02	4.23	8.26	13.68
(38) 1.25% 7/15/2020	78	46.04	1.55	0.005	0.001	0.00	2.45	-2.49	4.34
(39) 1.125% 1/15/2021	72	2.88	1.67	0.129	0.123	0.31	2.55	5.64	7.18
(40) 2.125% 2/15/2041+	71	1.25	0.52	0.494	1.346	0.03	2.81	2.37	4.05
(41) 0.125% 4/15/2016*	48	1.92	0.20	1.179	0.674	-0.11	3.16	9.22	12.09
(42) 0.625% 7/15/2021	66	3.60	2.00	0.074	0.062	0.21	2.59	-0.81	3.71
(43) 0.125% 1/15/2022	60	153.33	2.54	0.002	0.001	1.44	4.28	5.74	7.34
(44) 0.75% 2/15/2042+	59	1.43	1.16	0.534	2.089	0.34	2.81	3.03	4.61
(45) 0.125% 4/15/2017*	48	1.84	0.18	1.757	0.532	0.25	4.98	9.34	11.5
(46) 0.125% 7/15/2022	54	1.39	1.94	0.331	0.958	0.18	2.72	-0.91	3.50
(47) 0.125% 1/15/2023	48	1.40	1.26	0.614	1.685	0.39	3.42	5.56	6.49
(48) 0.625% 2/15/2043+	47	1.45	1.18	0.836	2.718	0.40	3.01	2.79	4.80
(49) 0.125% 4/15/2018*	45	1.94	0.34	1.434	0.777	0.08	4.98	11.44	12.70
(50) 0.375% 7/15/2023	42	1.11	1.63	0.555	2.494	0.27	3.25	-1.66	3.65
(51) 0.625% 1/15/2024	36	1.43	2.74	0.432	1.920	0.25	2.42	1.87	3.50
(52) 1.375% 2/15/2044+	35	1.68	1.06	2.796	4.020	0.50	1.78	6.26	6.78
(53) 0.125% 4/15/2019*	33	1.87	0.34	3.525	3.137	-0.05	2.71	11.69	12.09
(54) 0.125% 7/15/2024	30	1.39	3.64	0.247	1.172	-0.03	2.41	-5.44	6.30
(55) 0.25% 1/15/2025	24	2.05	6.74	0.178	0.945	0.12	1.90	-2.49	4.46
(56) 0.75% 2/15/2045+	23	1.64	1.34	9.981	6.919	0.43	1.66	5.34	5.70
(57) 0.125% 4/15/2020*	21	1.78	0.54	6.223	6.384	-0.19	2.98	9.78	10.31
(58) 0.375% 7/15/2025	18	0.95	5.70	0.411	5.780	-0.12	1.45	-8.37	8.74
(59) 0.625% 1/15/2026	12	30.93	8.74	0.007	0.009	-0.17	3.29	-7.58	9.14
(60) 1% 2/15/2046+	11	1.53	4.18	9.977	10.105	0.32	0.82	3.2	3.42
(61) 0.125% 4/15/2021*	9	1.60	0.85	7.948	11.139	0.13	1.74	6.15	6.36
(62) 0.125% 7/15/2026	6	11.79	10.21	0.094	0.141	0.31	1.16	-12.85	13.10
All TIPS		n.a.	n.a.	n.a.	n.a.	0.75	4.31	1.28	8.72

Table 3: **Estimated Liquidity Sensitivity Parameters and Fit for Individual TIPS**
The number of monthly observations and estimated T-O-L model parameters β^i and $\lambda^{L,i}$ for 62 TIPS. Mean errors and root mean squared errors (RMSE) of TIPS yields measured in basis points. The symbols *, †, and + indicate five-, twenty-, and thirty-year TIPS, respectively.

References

Abrahams, Michael, Tobias Adrian, Richard K. Crump, Emanuel Moench, and Rui Yu, 2016, "Decomposing Real and Nominal Yield Curves," *Journal of Monetary Economics*, Vol. 84, 182-200.

Andreasen, Martin M., Jens H. E. Christensen, and Simon Riddell, 2017, "The TIPS Liquidity Premium," Manuscript, Federal Reserve Bank of San Francisco.

Andreasen, Martin M., Jens H. E. Christensen, and Glenn D. Rudebusch, 2017, "Term Structure Modeling with Big Data," Manuscript, Federal Reserve Bank of San Francisco.

Bauer, Michael D., Glenn D. Rudebusch, and Jing (Cynthia) Wu, 2012, "Correcting Estimation Bias in Dynamic Term Structure Models," *Journal of Business and Economic Statistics*, Vol. 30, No. 3, 454-467.

Bernanke, Ben, 2005, "The Global Saving Glut and the U.S. Current Account Deficit," Sandridge Lecture, Richmond VA, March 10.

Campbell, John Y., Robert J. Shiller, and Luis M. Viceira, 2009, "Understanding Inflation-Indexed Bond Markets," *Brookings Papers on Economic Activity*, Spring, 79-120.

Carvalho, Carlos, Andrea Ferrero, and Fernanda Nechio, 2016, "Demographics and Real Interest Rates: Inspecting the Mechanism," *European Economic Review*, Vol. 88, 208-226.

Christensen, Jens H. E., Francis X. Diebold, and Glenn D. Rudebusch, 2011, "The Affine Arbitrage-Free Class of Nelson-Siegel Term Structure Models," *Journal of Econometrics*, Vol. 164, No. 1, 4-20.

Christensen, Jens H. E., Jose A. Lopez, and Glenn D. Rudebusch, 2010, "Inflation Expectations and Risk Premiums in an Arbitrage-Free Model of Nominal and Real Bond Yields," *Journal of Money, Credit and Banking*, Supplement to Vol. 42, No. 6, 143-178.

Christensen, Jens H. E., Jose A. Lopez, and Glenn D. Rudebusch, 2015, "A Probability-Based Stress Test of Federal Reserve Assets and Income," *Journal of Monetary Economics*, Vol. 73, 26-43.

Christensen, Jens H. E., Jose A. Lopez, and Patrick Shultz, 2017, "Do All New Treasuries Trade at a Premium?," *FRBSF Economic Letter*, 2017-03.

Christensen, Jens H. E. and Glenn D. Rudebusch, 2015, "Estimating Shadow-Rate Term Structure Models with Near-Zero Yields," *Journal of Financial Econometrics*, Vol. 13, No. 2, 226-259.

Clarida, Richard, 2014, "Navigating the New Neutral, " *Economic Outlook,* PIMCO, November.

Clark, Todd E. and Sharon Kozicki, 2005, "Estimating Equilibrium Real Interest Rates in Real Time," *The North American Journal of Economics and Finance*, Vol. 16, No. 3, 395-413.

Cúrdia, Vasco, Andrea Ferrero, Ging Cee Ng, and Andrea Tambalotti, 2015, "Has U.S. Monetary Policy Tracked the Efficient Interest Rate?," *Journal of Monetary Economics*, Vol. 70, 72-83.

Dai, Qiang and Kenneth J. Singleton, 2000, "Specification Analysis of Affine Term Structure Models," *Journal of Finance*, Vol. 55, No. 5, 1943-1978.

D'Amico, Stefania, Don H. Kim, and Min Wei, 2014, "Tips from TIPS: the Informational Content of Treasury Inflation-Protected Security Prices," Finance and Economics Discussion Series Working Paper 2014-24, Board of Governors of the Federal Reserve System.

Dudley, William C., Jennifer Roush, and Michelle Steinberg Ezer, 2009, "The Case for TIPS: An Examination of the Costs and Benefits," *Federal Reserve Bank of New York Economic Policy Review*, Vol. 15, No. 1, 1-17.

Duffee, Gregory R., 2002, "Term Premia and Interest Rate Forecasts in Affine Models," *Journal of Finance*, Vol. 57, No. 1, 405-443.

Duffie, Darrell and Rui Kan, 1996, "A Yield-Factor Model of Interest Rates," *Mathematical Finance*, Vol. 6, No. 4, 379-406.

Eggertsson, Gauti B., Neil R. Mehrotra, Sanjay R. Singh and Lawrence H. Summers, 2016, "A Contagious Malady? Open Economy Discussions of Secular Stagnation," *IMF Economic Review* Vol. 64, No. 4, 581-634.

Favero, Carlo A., Arie E. Gozluklu, and Haoxi Yang, 2016, "Demographics and the Behavior of Interest Rates " *IMF Economic Review* Vol. 64, No. 4, 732-776.

Fisher, Mark and Christian Gilles, 1996, "Term Premia in Exponential-Affine Models of the Term Structure," Manuscript, Board of Governors of the Federal Reserve System.

Fisher, Stanley, 2016, "Why Are Interest Rates So Low? Causes and Implications," Speech at the Economic Club of New York, New York, New York, October 17, https://www.federalreserve.gov/newsevents/speech/fischer20161017a.htm.

Fleckenstein, Mathias, Francis A. Longstaff, and Hanno Lustig, 2014, "The TIPS-Treasury Bond Puzzle," *Journal of Finance*, Vol. 69, No. 5, 2151-2197.

Fleming, Michael J. and Neel Krishnan, 2012, "The Microstructure of the TIPS Market," *Federal Reserve Bank of New York Economic Policy Review*, Vol. 18, No. 1, 27-45.

Gagnon, Etienne, Benjamin K. Johannsen, and David Lopez-Salido, 2016, "Understanding the New Normal: The Role of Demographics," Finance and Economics Discussion Series 2016-080. Washington: Board of Governors of the Federal Reserve System, http://dx.doi.org/10.17016/FEDS.2016.080.

Greenspan, Alan, 2005, Federal Reserve Board's Semiannual Monetary Policy Report to the Congress, Testimony to the U.S. Senate, February 16.

Grishchenko, Olesya V. and Jing-Zhi Huang, 2013, "Inflation Risk Premium: Evidence from the TIPS Market," *Journal of Fixed Income*, Vol. 22, No. 4, 5-30.

Gürkaynak, Refet S., Brian Sack, and Jonathan H. Wright, 2007, "The U.S. Treasury Yield Curve: 1961 to the Present," *Journal of Monetary Economics*, Vol. 54, No. 8, 2291-2304.

Gürkaynak, Refet S., Brian Sack, and Jonathan H. Wright, 2010, "The TIPS Yield Curve and Inflation Compensation," *American Economic Journal: Macroeconomics*, Vol. 2, No. 1, 70-92.

Hall, Robert E., 2016, "The Role of the Growth of Risk-Averse Wealth in the Decline of the Safe Real Interest Rate," Manuscript, Stanford University.

Hamilton, James D., Ethan S. Harris, Jan Hatzius, and Kenneth D. West, 2016, "The Equilibrium Real Funds Rate: Past, Present, and Future " *IMF Economic Review* Vol. 64, No. 4, 660-707.

Holston, Kathryn, Thomas Laubach, and John C. Williams, 2017, "Measuring the Natural Rate of Interest: International Trends and Determinants," *Journal of International Economics*, in press, http://dx.doi.org/10.1016/j.jinteco.2017.01.004.

Hu, Grace Xing, Jun Pan, and Jiang Wang, 2013, "Noise as Information for Illiquidity," *Journal of Finance*, Vol. 68, No. 6, 2341-2382.

Johannsen, Benjamin K., and Elmar Mertens, 2016. "A Time Series Model of Interest Rates with the Effective Lower Bound," Finance and Economics Discussion Series 2016-033, Washington: Board of Governors of the Federal Reserve System.

Kaminska, Iryna, and Gabriele Zinna, 2014. "Official Demand for U.S. Debt: Implications for U.S. Real Interest Rates," IMF Working Paper 14/66, Washington: International Monetary Fund.

Kiley, Michael T., 2015, "What Can the Data Tell Us About the Equilibrium Real Interest Rate?," Working Paper Finance and Economics Discussion Series 2015-077, Board of Governors of the Federal Reserve System.

Kim, Don H. and Kenneth J. Singleton, 2012, "Term Structure Models and the Zero Bound: An Empirical Investigation of Japanese Yields," *Journal of Econometrics*, Vol. 170, No. 1, 32-49.

Laubach, Thomas and John C. Williams, 2003, "Measuring the Natural Rate of Interest," *Review of Economics and Statistics*, Vol. 85, No. 4, 1063-1070.

Laubach, Thomas and John C. Williams, 2016, "Measuring the Natural Rate of Interest Redux," *Business Economics*, Vol. 51, No. 2, 57-67.

Lo, Stephanie and Kenneth Rogoff, 2015, "Secular Stagnation, Debt Overhang and Other Rationales for Sluggish Growth, Six Years On," Bank for International Settlements, Working Paper No. 482.

Lubik, Thomas A., and Christian Matthes, 2015, "Calculating the Natural Rate of Interest: A Comparison of Two Alternative Approaches," Federal Reserve Bank of Richmond Economic Brief, EB15-10.

Orphanides, Athanasios, and John C. Williams, 2002, "Robust Monetary Policy Rules with Unknown Natural Rates," *Brookings Papers on Economic Activity* 2002(2), 63-145.

Pescatori, Andrea and Jarkko Turunen, 2016, "Lower for Longer: Neutral Rate in the U.S.," *IMF Economic Review* Vol. 64, No. 4, 708-731.

Pflueger, Carolin E. and Luis M. Viceira, 2013, "Return Predictability in the Treasury Market: Real Rates, Inflation, and Liquidity," Manuscript, Harvard University.

Rachel, Lukasz, and Thomas D Smith, 2015, "Secular Drivers of the Global Real Interest Rate," Staff working paper 571, Bank of England.

Rudebusch, Glenn D., 2001, "Is the Fed Too Timid? Monetary Policy in an Uncertain World," *Review of Economics and Statistics* Vol. 83, No. 2, 203-217.

Rudebusch, Glenn D. and Lars Svensson, 1999, "Policy Rules for Inflation Targeting," In *Monetary Policy Rules*, ed. by Taylor, Chicago: University of Chicago Press, 203-246.

Rudebusch, Glenn D. and Eric Swanson, 2011, "The Bond Premium in a DSGE Model with Long-Run Real and Nominal Risks," *American Economic Journals: Macroeconomics*, Vol. 4, No. 1, 105-43.

Sack, Brian and Robert Elsasser, 2004, "Treasury Inflation-Indexed Debt: A Review of the U.S. Experience," *Federal Reserve Bank of New York Economic Policy Review*, Vol. 10, No. 1, 47-63.

Summers, Lawrence H., 2014, "U.S. Economic Prospects: Secular Stagnation, Hysteresis, and the Zero Lower Bound," *Business Economics*, Vol. 49, No. 2, 65-73.

Summers, Lawrence H., 2015, "Demand Side Secular Stagnation, " *American Economic Review, Papers and Proceedings* Vol. 105, No. 5, 60-65.

Swanson, Eric T. and John C. Williams, 2014, "Measuring the Effect of the Zero Lower Bound on Medium- and Longer-Term Interest Rates," *American Economic Review*, Vol. 104, No. 10, 3154-3185.

Taylor, John B., and Volker Wieland, 2016, "Finding the Equilibrium Real Interest Rate in a Fog of Policy Deviations," Discussion paper 11264, Centre for Economic Policy Research.

Williams, John C., 2016, "Monetary Policy in a Low R-star World," *FRBSF Economic Letter* 2016-23, Federal Reserve Bank of San Francisco, August 15.

Yellen, Janet, 2015, "Normalizing Monetary Policy: Prospects and Perspectives," Speech at the Federal Reserve Bank of San Francisco, San Francisco, California, March 27, 2015.